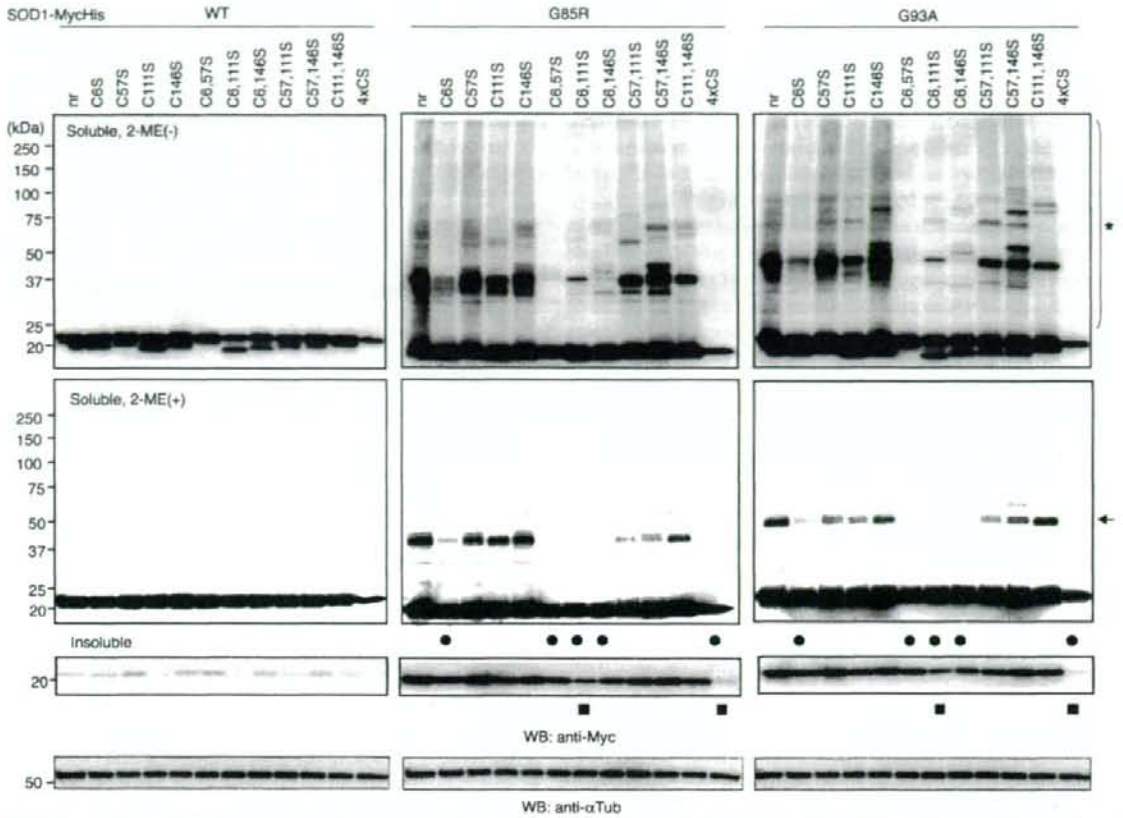

FIGURE 2. **Free Cys^6 and Cys^{111} are important for generating intermolecular disulfide-linked species and insoluble, sedimentable forms of mutant human SOD1.** Various combinations of replacing Cys with Ser were introduced into wild-type (*WT*) and mutant (G85R and G93A) SOD1-MycHis. Neuro-2a cells expressing SOD1-MycHis were treated with 2 μM MG132 for 24 h. Soluble fractions were analyzed by SDS-PAGE in the absence (*upper panels*) or presence (*middle panels*) of 2-ME. Insoluble fractions were analyzed by SDS-PAGE in the presence of 2-ME (*lower panels*). *Asterisk*, a disulfide-linked high molecular weight species; *arrow*, an SDS-resistant dimer of mutant SOD1. *Filled circles*, marked reduction of an SDS-resistant dimer with a Cys^6 replacement of mutant SOD1; *filled squares*, further reduction of the detergent-insoluble, sedimentable form of mutant SOD1 with simultaneous Cys^6 and Cys^{111} replacements. *nr*, SOD1 without replacement in cysteine residue; *4×CS*, all four cysteines replaced by serines.

amino acids changes by the anti-SOD1 antibody. Interestingly, none of the Cys residue replacements generated disulfide-linked species in wild-type SOD1 proteins (Fig. 2, *left panel*). Under reducing conditions, replacement of Cys^6 had a stronger effect on the formation of disulfide-linked species of mutant SOD1 than did the other three Cys residue replacements (Fig. 2, *middle* and *right panels*, *asterisk*). Combinations of replacing Cys^6 and one of the other Cys residues further attenuated the aberrant disulfide-linking of mutant SOD1 seen with the single substitution of Cys^6 (Fig. 2, *filled circle*). Under usual reducing conditions, the same reduced oligomerization of mutant SOD1 was observed when combinations of Cys^6 and other Cys residues were replaced (Fig. 2, *arrow*). The detergent-insoluble, sedimentable form of mutant SOD1 was also reduced especially if both Cys^6 and Cys^{111} were replaced (Fig. 2, *filled square*). Replacement of all four Cys residues completely abolished the disulfide-linked species in the non-reducing condition and the oligomeric, detergent-insoluble form of mutant SOD1 in the reducing condition (Fig. 2, *lane 4×CS*). Because simultaneous substitutions of Cys^6 and Cys^{111} had the strongest effects on the formation of aberrant species of mutant SOD1 in both non-reducing and reducing conditions, we compared C6S and C111S mutants with C57S and C146S mutants in the following experiments.

Substituting Both Cys^6 and Cys^{111} Greatly Reduces High Molecular Weight Aggregate Formation and Ubiquitylation of Mutant SOD1—In studies of polyglutamine disorders, it has been demonstrated that high molecular weight aggregates of mutant proteins are retained by filtration through cellulose acetate (25, 26). Cellulose acetate membranes usually bind protein very poorly and are used to trap high molecular weight structures from complex mixtures through filtration. This assay was also successfully applied to detect mutant SOD1 aggregation (27). Thus we used a cellulose acetate filter trap assay to investigate whether SOD1 proteins with Cys substitutions are retained in high molecular weight aggregates from lysates of SOD1-MycHis expressing Neuro-2a cells. Cells were lysed in TNE buffer, fractionated into crude denucleated, soluble, and insoluble fractions, and each fraction was then filtered through a 0.22-μm cellulose acetate membrane. Subsequent staining

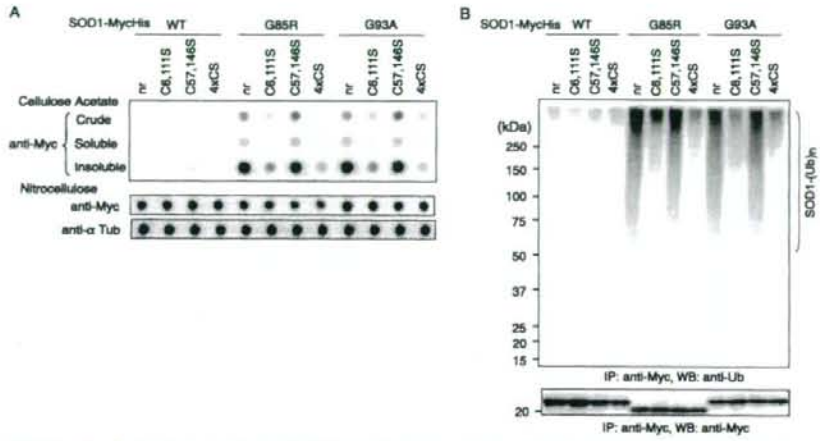

FIGURE 3. **Replacing both Cys^6 and Cys^{111} greatly reduces high molecular weight aggregate formation and ubiquitylation of mutant SOD1-MycHis.** *A*, crude, soluble, and insoluble fractions of cell lysates were analyzed by filter trap assay (*upper panel*). Nitrocellulose dot blots probed with anti-Myc (*middle panel*) and anti-α-tubulin (*lower panel*) antibodies were used as loading controls. *B*, *in vivo* ubiquitylation assay. Western blotting of SOD1-Myc-His immunoprecipitates with anti-ubiquitin antibody demonstrated polyubiquitylation of mutant SOD1s and their C57, 146S derivatives. Replacement of Cys^6 and Cys^{111} abolished polyubiquitylation of mutant SOD1. *nr*, SOD1 without replacement in cysteine residue; *4×CS*, all four cysteines replaced by serines.

with anti-Myc antibody revealed trapped SOD1 proteins (Fig. 3*A*, *upper panel*). Interestingly, high molecular weight aggregates were abundantly detected in mutant SOD1^{G85R}, SOD1^{G93A}, and their C57S and C146S derivatives. Replacements of Cys^6 and Cys^{111} greatly reduced high molecular weight structures of mutant SOD1. No high molecular weight aggregates were present in either wild-type SOD1 or their Cys-substituted mutants.

Mutant, but not wild-type, SOD1 is conjugated to a multiubiquitin chain and degraded at the proteasome (20, 28). To assess whether SOD1 proteins are ubiquitylated, we carried out an *in vivo* ubiquitylation analysis by expressing SOD1^{WT}, SOD1^{G85R}, SOD1^{G93A}, and their Cys to Ser mutants in Neuro-2a cells in the presence of the proteasome inhibitor MG132. When SOD1 was then immunoprecipitated, mutant SOD1s, but not wild-type SOD1, were polyubiquitylated (Fig. 3*B*, *lane 1*). Replacement of both Cys^6 and Cys^{111} abolished ubiquitylation of mutant SOD1, whereas replacement of Cys^{57} and Cys^{146} did not affect the ubiquitylation status of mutant SOD1 (Fig. 3*B*, *lane 2 versus lane 3*). Wild-type SOD1 and its Cys-replacement mutants were not ubiquitylated at all. Replacing only one of the four Cys residues attenuated neither the formation of high molecular weight species nor the ubiquitylation of mutant SOD1 (data not shown). Thus, the presence of both Cys^6 and Cys^{111} is important for high molecular weight aggregate formation and ubiquitylation of mutant SOD1. Disulfide bond formation at Cys^6 or Cys^{111} is critical step for ubiquitylation of mutant SOD1.

Formation of Disulfide-linked Species of Mutant SOD1 Strongly Correlates with Visible Aggregate Formation and Neurotoxicity—Expression of mutant, but not wild-type, SOD1 induces large perinuclear intracytoplasmic aggregates in differentiated Neuro-2a cells and reduces cellular viability (20). We analyzed the role of mutant SOD1 Cys residues in aggregate formation and neurotoxicity in Neuro-2a cells. Replacements of Cys^6 and Cys^{111} significantly reduced the percentage of mutant SOD1^{G85R} and SOD1^{G93A} cells with visible aggregates (Fig. 4*A*). To further demonstrate the extent of aggregate formation, we isolated SOD1 aggregates with a procedure according to Lee *et al.* (24). Differentiated Neuro-2a cells bearing SOD1-GFP aggregates were extracted with 1% Nonidet P-40 in the culture dish, and the Nonidet P-40-soluble proteins were gently removed. Under this condition, the soluble monomeric SOD1 was completely removed, and the aggregates remained in the culture dish due to their association with unknown structures (24). The remaining Nonidet P-40-insoluble portion was then scraped and centrifuged at 80 × *g*. After the centrifugation at 80 × *g* for 15 min, the pellet fraction was found to contain exclusively the large inclusion bodies. Replacements of Cys^6 and Cys^{111} markedly reduced the number of inclusion bodies in G93A mutant SOD1-GFP (Fig. 4*B*). Mutant SOD1^{G85R} and SOD1^{G93A}, but not wild-type SOD1, are toxic in differentiated Neuro-2a cells as previously described (20). However, replacement of the Cys^6 and Cys^{111} residues markedly reduced this neurotoxicity (Fig. 4*C*), which was not affected by replacing the Cys^{57} and Cys^{146} residues. There were no significant differences among the expression levels of all the constructs (Fig. 4*D*). Thus, changes in inclusion formation and toxicity are not due to differences in altered expression. These results provide evidence of direct links among intermolecular disulfide bonding, ubiquitylated complex formation, visible aggregate formation, and neurotoxicity.

Preferential Occurrence of Disulfide-cross-linked Mutant SOD1 in the Affected Lesions of ALS Model Mice—Although mutant SOD1 is expressed at similar levels in both neuronal and non-neuronal tissues, the aggregated and ubiquitylated forms are selectively found in the pathological lesions of patients and mutant SOD1-transgenic mice (29, 30). Thus, we next examined whether mutant SOD1 is aberrantly disulfide-linked in various tissues from symptomatic mutant SOD1 transgenic mice. Western blotting analysis, using anti-SOD1 antibody under reducing and non-reducing (omitting reducing agent 2-ME) conditions, demonstrated that the expression levels of mutant SOD1 were nearly the same in all tissues examined. Each of the tissues showed some of the disulfide-linked mutant SOD1species; however, in the brain stem and spinal cord, the areas predominantly affected in mutant SOD1-linked ALS, there was increased formation of intermolecular disulfide-linked species of mutant SOD1 (Fig. 5). Thus, intermolecular disulfide-linked

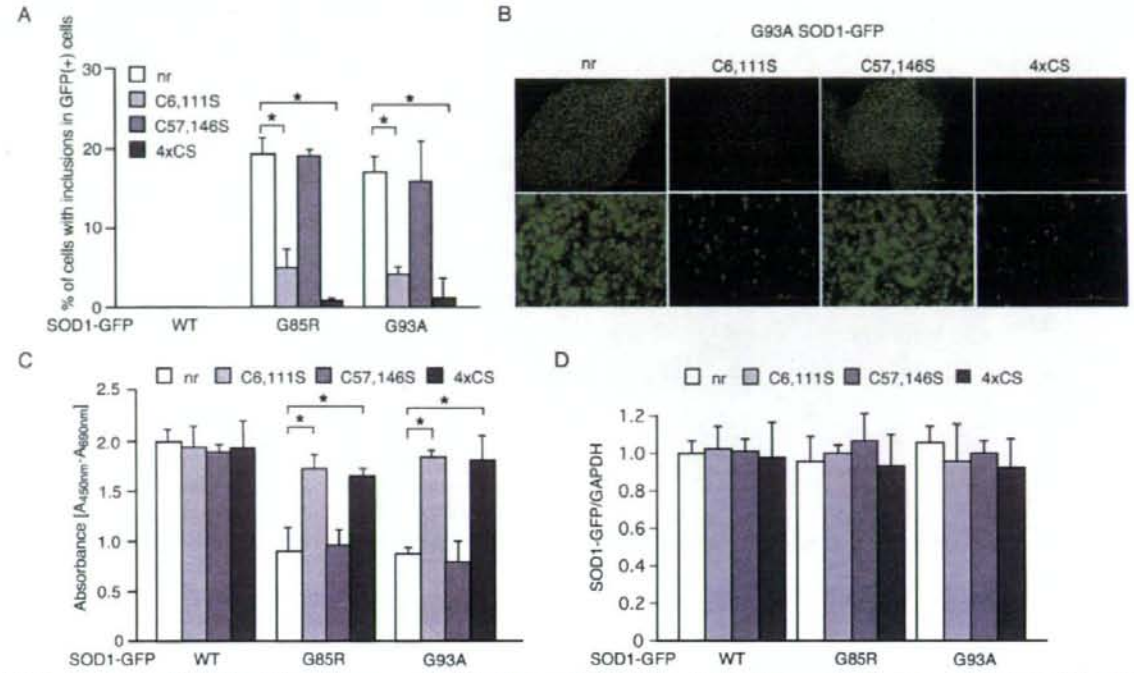

FIGURE 4. **Formation of disulfide-linked species of mutant SOD1 strongly correlates with visible aggregate formation and neurotoxicity.** *A*, the frequency of inclusion-bearing cells transfected with wild-type (*WT*), G85R, and G93A mutant SOD1-GFP and their Cys to Ser derivatives. *B*, G93A mutant SOD1-GFP inclusion bodies in 80 × *g* pellet. *Lower panels* are a high magnification image of the portion on the *upper panels* showing the whole pellet. The *scale bar* is equivalent to 10 mm in the *upper panels*, and 200 μm in the *lower panels*. *C*, change in the neurotoxic effect of mutant SOD1-GFP by Cys replacements to Ser. Cell viability was measured by the WST-1-based assay. *D*, all the constructs have equal expression. Transcription levels of SOD1-GFP in Neuro-2a cells expressing WT, G85R, and G93A mutant SOD1 and their Cys to Ser derivatives were examined by quantitative reverse transcription-PCR. Data were normalized with glyceraldehyde-3-phosphate dehydrogenase expression and then represent relative expression levels compared with levels in cells expressing WT SOD1-GFP. Data are mean ± S.D. values of triplicate assays. Statistical analyses were carried out by analysis of variance. *, $p < 0.01$. *nr*, SOD1 without replacing cysteine residues; *4×CS*, all four cysteines replaced by serines.

species are implicated as the aggregation-prone and neurotoxic intermediate of mutant SOD1 *in vivo*.

Effects of Cys^{6}- and Cys^{111}-mediated Disulfide Linking on the Rate of Mutant SOD1 Degradation—To determine whether replacement of Cys residues affects the degradation of SOD1 proteins, we examined the stability of mutant SOD1 proteins expressed in Neuro-2a cells (Fig. 6, *A* and *B*). Chase experiments with cycloheximide, which halts all cellular protein synthesis, demonstrated that replacement of Cys residues did not influence the stability of wild-type SOD1 protein (Fig. 6*A*). By contrast, although mutant SOD1 showed the enhanced degradation compared with wild-type proteins previously described (18–20), when both Cys^{6} and Cys^{111} were replaced with Ser, the degradation of mutant SOD1 was markedly increased (Fig. 6*B*). Replacement of Cys^{57} and Cys^{146} did not significantly change the rate of degradation compared with Cys-native mutant SOD1 protein.

Ubiquityl Ligase Dorfin Ubiquitylates and Promotes Degradation of Disulfide-linked Mutant SOD1—We have previously shown that Dorfin physically binds and ubiquitylates various familial ALS-linked SOD1 mutants and enhances their degradation (20). Thus, we examined whether Cys residues on SOD1 affect the binding and ubiquitylating activities of Dorfin. To this end, Dorfin was co-expressed with wild-type or mutant SOD1 in Neuro-2a cells. Dorfin co-immunoprecipitated with G85R and G93A mutant SOD1s and their Cys^{57}- and Cys^{146}-replaced derivatives (Fig. 7*A*). However, Dorfin interacted with Cys^{6}- and Cys^{111}-replaced mutant SOD1 only very weakly and failed to bind to mutant SOD1 when all four Cys residues were replaced (Fig. 7*A*). Dorfin did not bind at all to wild-type SOD1. Using an *in vivo* ubiquitylation assay, we further examined whether co-expressed Dorfin enhances the ubiquitylation of Cys-substituted mutant SOD1 (Fig. 7*B*). When Cys-native or Cys^{57}- and Cys^{146}-replaced mutant SOD1s were co-expressed with Dorfin, ubiquitylation of mutant SOD1s were increased; however, co-expression of Dorfin with mutant SOD1 in which Cys^{6} and Cys^{111} or all four Cys residues were replaced did not promote ubiquitylation of these mutant SOD1s (Fig. 7*B*). Chase experiments with cycloheximide in the presence or absence of Dorfin demonstrated that degradation of Cys-native and Cys^{57}- and Cys^{146}-replaced mutant SOD1^{G93A} was greatly accelerated when Dorfin was overexpressed, whereas the stability of Cys^{6} and Cys^{111} or all four Cys-replaced mutant SOD1G93A were unaffected (Fig. 7*C*). We have previously shown that Dorfin exerts neuroprotective effects by promoting degradation of mutant SOD1 through its ubiquityl ligase activities (20). Co-expression of Dorfin improved the viability of Neuro-2a cells expressing Cys-

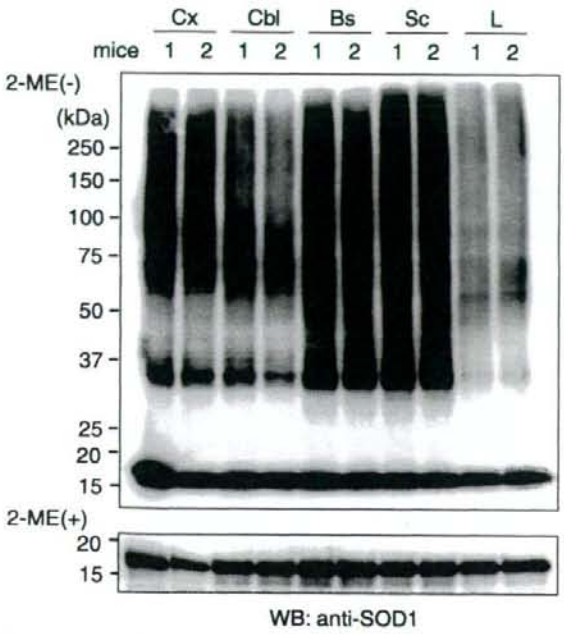

FIGURE 5. **Preferential occurrence of disulfide-cross-linked mutant SOD1 in the affected lesion of ALS model mice.** Western blotting of tissue samples from two 17-week-old symptomatic G93A mutant SOD1-transgenic mice under non-reducing (*upper panel*) and reducing (*lower panel*) conditions. *Cx*, cerebral cortex; *Cbl*, cerebellum; *Bs*, brain stem; *Sc*, spinal cord; *L*, liver.

native and Cys[57]- and Cys[146]-replaced mutant SOD1[G93A] (Fig. 7*D*).

DISCUSSION

Mutations in the *SOD1* gene cause familial ALS through the gain of a toxic function, however, the nature of this toxic function remains largely unknown (31). Ubiquitylated aggregates of mutant SOD1 proteins in affected lesions are a pathological hallmark of the disease (32) and suggest their relation to neurotoxicity. Recent biochemical studies suggest that the immature disulfide-reduced forms of the familial ALS mutant SOD1 proteins play a critical role in this neurotoxicity; *in vitro*, these forms tend to misfold, oligomerize, and readily undergo incorrect disulfide bond formation upon mild oxidative stress (16, 33). Among the more than 100 ALS-associated human SOD1 mutants, some cannot intrinsically form the essential intramolecular disulfide bonds. One of the conserved Cys residues, Cys[146], is missing in some of the mutants, such as the Leu[126] del TT (stop at 131) and Gly[127] ins TGGG (stop at 133); however, it has been reported that minute quantities of SOD1 aggregates can cause the disease in mice expressing the truncated mutant, Gly[127] ins TGGG (stop at 133) (34). Furthermore, a significant fraction of the insoluble SOD1 aggregates in the spinal cord of ALS model mice contain multimers cross-linked via intermolecular disulfide bonds (17, 35). In the present study, we showed that non-physiological intermolecular disulfide bonds involving Cys[6] and Cys[111] of the mutant SOD1 were important for high molecular weight aggregate formation, ubiquitylation, and neurotoxicity *in vivo*, all of which were dramatically reduced in Neuro-2a cells when these residues were replaced with serines.

Human SOD1 has two free cysteine residues, Cys[6] and Cys[111] (36). Cys[6] is located adjacent to the dimer interface pointed toward the interior of the β-barrel and is solute-inaccessible in the native, folded conformation. Cys[111] is located near the surface and is solute-accessible and -reactive, often becoming blocked during purification (37). Replacement of the free Cys residues increased the resistance to thermal inactivation (38). Increased resistance of mutant SOD1s is due to increased resistance to irreversible unfolding and relatively unaffected by changes in conformational stability (39). Our data, showing that aggregate formation of mutant SOD1 is reduced when Cys[6] and Cys[111] are replaced with serines, are compatible with these observations. Mutations of the Cys[6] residue (C6F and C6G) still result in familial ALS (4), and in a transgenic mouse expressing mouse SOD1 retaining cystines 6, 57, and 146 but lacking

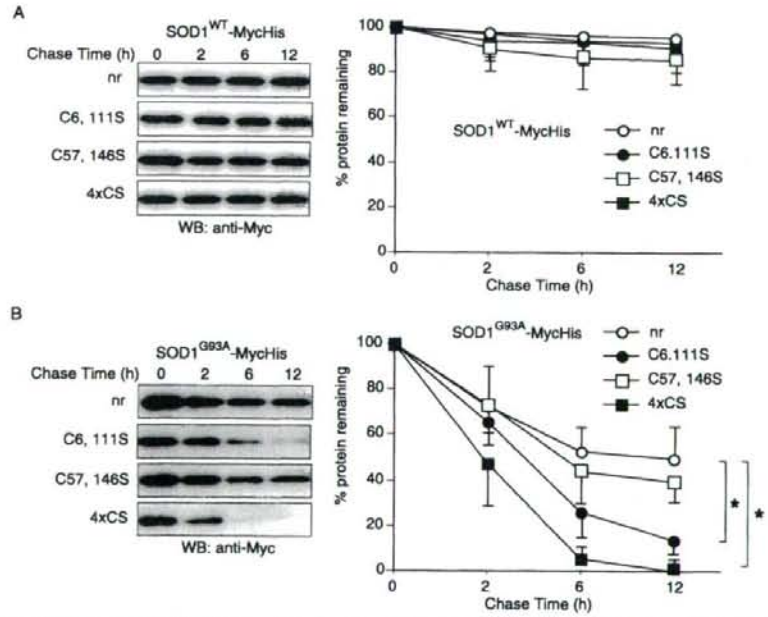

FIGURE 6. **Effects of disulfide-linking at Cys[6] and Cys[111] on the rate of mutant SOD1 degradation.** Cycloheximide chase analysis on Neuro-2a cells expressing (*A*) wild-type (*WT*) and (*B*) G93A mutant SOD1 and their Cys to Ser derivatives. Western blots showing levels of SOD1 protein at various times after the cycloheximide chase are in the *left panels*. Quantitative data on the right are mean ± S.D. values of three independent experiments. Statistical analyses were carried out by analysis of variance. *, $p < 0.01$. *nr*, SOD1 without cysteine residue replacement; *4×CS*, all four cysteines replaced by serines.

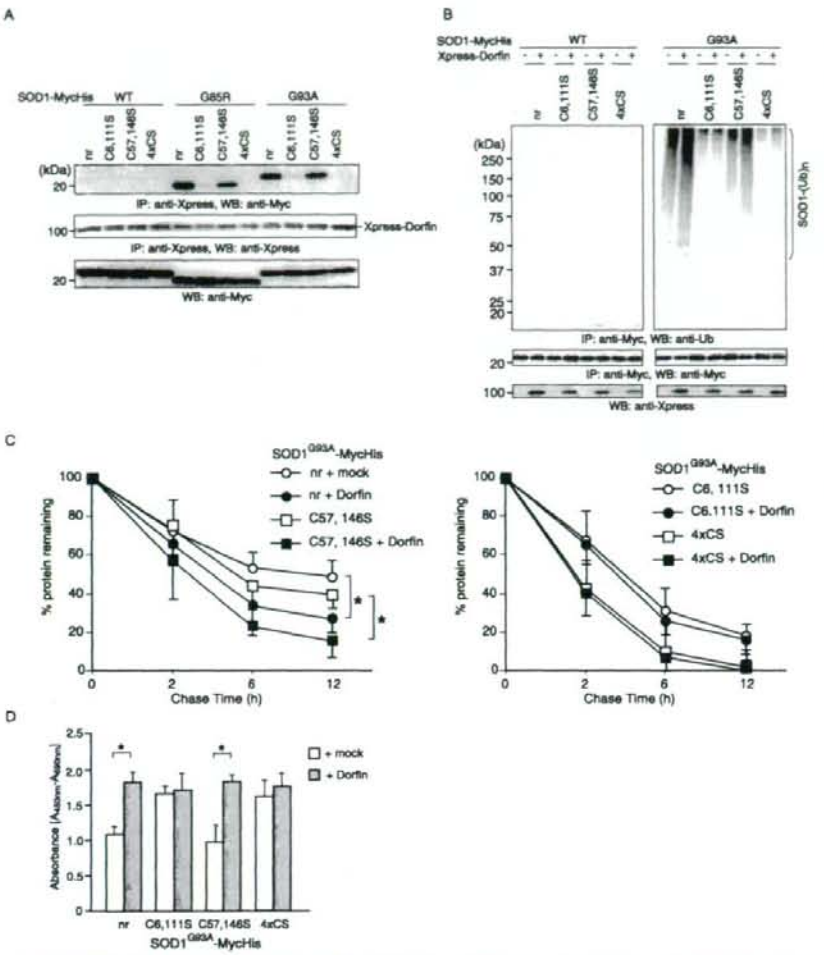

FIGURE 7. **Ubiquityl ligase Dorfin binds, ubiquitylates, and promotes degradation of disulfide-linked mutant SOD1.** *A*, replacement of Cys^6 and Cys^{111} nearly eliminated the interaction of Dorfin with mutant SOD1. Various SOD1-MycHis were co-transfected with Xpress-Dorfin. After immunoprecipitation with anti-Xpress antibody, the resulting precipitates and cell lysates were analyzed by Western blotting with anti-Myc antibody. *B, in vivo*, Dorfin failed to promote ubiquitylation of mutant SOD1 with the Cys^6 and Cys^{111} replacement. Western blotting of SOD1-Myc-His immunoprecipitates with anti-ubiquitin antibody. *C*, Dorfin failed to promote degradation of mutant SOD1 with both Cys^6 and Cys^{111} replaced. Cycloheximide chase analysis of G93A mutant SOD1 with Cys^6 and Cys^{111}-replacements (*left panel*) or with Cys^{57} and Cys^{146}-replacements (*right panel*) in the presence or absence of overexpressed Xpress-Dorfin. *D*, Dorfin prevented neurotoxicity by mutant SOD1 with intact Cys^6 and Cys^{111} residues. Cell viability was measured by the WST-1-based assay. Data are mean ± S.D. values of three independent experiments. Statistical analyses were carried out by unpaired *t* test. *, $p < 0.01$. *nr*, SOD1 without replacement in cysteine residue; *4×CS*, all four cysteines replaced by serines.

111 and with a G86R mutation corresponding to G85R mutation in human SOD1, degeneration of motor neurons in the spinal cord has been observed (40). These results imply that, if one of either the Cys^6 or Cys^{111} residues is present, it can still be a disease-causing SOD1. Our data here also revealed that replacement of only one of the Cys residues at positions 6 or 111 had modest effects on the formation of aggregates (Fig. 2).

Cytoplasmic proteins are degraded mainly via two pathways, the ubiquitin-proteasome pathway (6) and via autophagy (7). Previous studies have shown that mutant SOD1 proteins are turned over more rapidly than wild-type SOD1 (12, 18, 19). Two distinct ubiquitin ligases, Dorfin and NEDL1, were reported to specifically ubiquitylate mutant but not wild-type SOD1 (20, 21). These studies suggest that mutant SOD1 is degraded by the ubiquitin-proteasome pathway and that the accelerated turnover of mutant SOD1 is mediated in part by this pathway. Impairment of the proteasome activities may contribute to ALS pathogenesis (28, 41, 42). We showed here that proteasome inhibition led to a dose-dependent accumulation of aberrant disulfide-linked high molecular weight mutant SOD1 (Fig. 1), suggesting that disulfide-linking mediates ubiquitylation of mutant SOD1. In fact, we found that Dorfin ubiquitylated mutant SOD1 by recognizing the Cys^6 and Cys^{111} disulfide cross-linked form and targeted it for proteasomal degradation (Fig. 7). Mutant SOD1, in which the Cys^6 and Cys^{111} were replaced, was not ubiquitylated (Fig. 3), and its rate of degradation was not affected in the presence of Dorfin (Fig. 7). It is possible that mutant SOD1 lacking Cys^6 and Cys^{111} may be degraded directly by the proteasome without ubiquitylation (43) or by autophagy (44), but further studies are needed to address this issue.

The appearance of mutant SOD1 aggregates in motor neurons of familial ALS patients and mouse models has suggested that aggregation plays an important role in neurotoxicity (31). However, conflicting results have been reported on the correlation between aggregate formation and cell death. One report showed that aggregate formation of mutant $SOD1^{A4V}$ and $SOD1^{V148G}$ does not correlate with cell death (45), whereas another study using live cell-imaging techniques reported that the ability of mutant $SOD1^{G85R}$ and $SOD1^{G93A}$ proteins to form aggregates directly correlates with neuronal cell death (46). These controversies also exist in other neurodegenerative diseases (47, 48). In this study, we clearly showed a direct link among intermolecular disulfide bond-mediated high molecular weight complex formation, visible aggregate formation, and neurotoxicity (Figs. 2–4).

Furukawa *et al.* (16) reported that formation of disulfide-linked multimers need not involve the non-conserved Cys residues, Cys^6 and Cys^{111}, and that the conserved Cys residues, Cys^{57} and Cys^{146}, play an important role in the apo-form of

SOD1 multimerization upon oxidative stress. Our results underscore the importance of Cys^{6} and Cys^{111} for high molecular weight aggregate formation, ubiquitylation, and neurotoxicity in Neuro-2a cells. This discrepancy may result from differences in experimental conditions; we studied human SOD1 proteins expressed in Neuro-2a cells, and Furukawa *et al.* used the purified apo-form of human SOD1 from *Escherichia coli*. Further studies will clarify the roles of each of the Cys residues of the mutant SOD1 protein in the ALS pathogenesis *in vivo* by generating transgenic mice bearing mutant SOD1 lacking Cys^{6} and Cys^{111} or Cys^{57} and Cys^{146}.

REFERENCES

1. McCord, J. M., and Fridovich, I. (1969) *J. Biol. Chem.* **244,** 6049–6055
2. Fridovich, I. (1974) *Adv. Enzymol. Relat. Areas. Mol. Biol.* **41,** 35–97
3. Rosen, D. R. (1993) *Nature* **364,** 362
4. Valentine, J. S., Doucette, P. A., and Potter, S. Z. (2005) *Annu. Rev. Biochem.* **74,** 563–593
5. Crapo, J. D., Oury, T., Rabouille, C., Slot, J. W., and Chang, L. Y. (1992) *Proc. Natl. Acad. Sci. U. S. A.* **89,** 10405–10409
6. Fridovich, I. (1986) *Adv. Enzymol. Relat. Areas. Mol. Biol.* **58,** 61–97
7. Fisher, C. L., Cabelli, D. E., Tainer, J. A., Hallewell, R. A., and Getzoff, E. D. (1994) *Proteins* **19,** 24–34
8. Arnesano, F., Banci, L., Bertini, I., Martinelli, M., Furukawa, Y., and O'Halloran, T. V. (2004) *J. Biol. Chem.* **279,** 47998–48003
9. Freedman, R. B. (1995) *Curr. Opin. Struct. Biol.* **5,** 85–91
10. Lindenau, J., Noack, H., Possel, H., Asayama, K., and Wolf, G. (2000) *Glia* **29,** 25–34
11. Tiwari, A., and Hayward, L. J. (2003) *J. Biol. Chem.* **278,** 5984–5992
12. Borchelt, D. R., Lee, M. K., Slunt, H. S., Guarnieri, M., Xu, Z. S., Wong, P. C., Brown, R. H., Jr., Price, D. L., Sisodia, S. S., and Cleveland, D. W. (1994) *Proc. Natl. Acad. Sci. U. S. A.* **91,** 8292–8296
13. Ratovitski, T., Corson, L. B., Strain, J., Wong, P., Cleveland, D. W., Culotta, V. C., and Borchelt, D. R. (1999) *Hum. Mol. Genet* **8,** 1451–1460
14. Rakhit, R., Crow, J. P., Lepock, J. R., Kondejewski, L. H., Cashman, N. R., and Chakrabartty, A. (2004) *J. Biol. Chem.* **279,** 15499–15504
15. Doucette, P. A., Whitson, L. J., Cao, X., Schirf, V., Demeler, B., Valentine, J. S., Hansen, J. C., and Hart, P. J. (2004) *J. Biol. Chem.* **279,** 54558–54566
16. Furukawa, Y., and O'Halloran, T. V. (2005) *J. Biol. Chem.* **280,** 17266–17274
17. Furukawa, Y., Fu, R., Deng, H. X., Siddique, T., and O'Halloran, T. V. (2006) *Proc. Natl. Acad. Sci. U. S. A.* **103,** 7148–7153
18. Hoffman, E. K., Wilcox, H. M., Scott, R. W., and Siman, R. (1996) *J. Neurol. Sci.* **139,** 15–20
19. Johnston, J. A., Dalton, M. J., Gurney, M. E., and Kopito, R. R. (2000) *Proc. Natl. Acad. Sci. U. S. A.* **97,** 12571–12576
20. Niwa, J., Ishigaki, S., Hishikawa, N., Yamamoto, M., Doyu, M., Murata, S., Tanaka, K., Taniguchi, N., and Sobue, G. (2002) *J. Biol. Chem.* **277,** 36793–36798
21. Miyazaki, K., Fujita, T., Ozaki, T., Kato, C., Kurose, Y., Sakamoto, M., Kato, S., Goto, T., Itoyama, Y., Aoki, M., and Nakagawara, A. (2004) *J. Biol. Chem.* **279,** 11327–11335
22. Niwa, J., Ishigaki, S., Doyu, M., Suzuki, T., Tanaka, K., and Sobue, G. (2001) *Biochem. Biophys. Res. Commun.* **281,** 706–713
23. Marin, I., and Ferrus, A. (2002) *Mol. Biol. Evol.* **19,** 2039–2050
24. Lee, H. J., and Lee, S. J. (2002) *J. Biol. Chem.* **277,** 48976–48983
25. Scherzinger, E., Lurz, R., Turmaine, M., Mangiarini, L., Hollenbach, B., Hasenbank, R., Bates, G. P., Davies, S. W., Lehrach, H., and Wanker, E. E. (1997) *Cell* **90,** 549–558
26. Bailey, C. K., Andriola, I. F., Kampinga, H. H., and Merry, D. E. (2002) *Hum. Mol. Genet.* **11,** 515–523
27. Wang, J., Xu, G., and Borchelt, D. R. (2002) *Neurobiol. Dis.* **9,** 139–148
28. Urushitani, M., Kurisu, J., Tsukita, K., and Takahashi, R. (2002) *J. Neurochem.* **83,** 1030–1042
29. Gurney, M. E., Pu, H., Chiu, A. Y., Dal Canto, M. C., Polchow, C. Y., Alexander, D. D., Caliendo, J., Hentati, A., Kwon, Y. W., Deng, H. X., Chen, W., Zhai, P., Sufit, R. L., and Siddique, T. (1994) *Science* **264,** 1772–1775
30. Bruijn, L. I., Houseweart, M. K., Kato, S., Anderson, K. L., Anderson, S. D., Ohama, E., Reaume, A. G., Scott, R. W., and Cleveland, D. W. (1998) *Science* **281,** 1851–1854
31. Cleveland, D. W., and Rothstein, J. D. (2001) *Nat. Rev. Neurosci.* **2,** 806–819
32. Watanabe, M., Dykes-Hoberg, M., Culotta, V. C., Price, D. L., Wong, P. C., and Rothstein, J. D. (2001) *Neurobiol. Dis.* **8,** 933–941
33. Wang, J., Xu, G., and Borchelt, D. R. (2006) *J. Neurochem.* **96,** 1277–1288
34. Jonsson, P. A., Graffmo, K. S., Andersen, P. M., Brannstrom, T., Lindberg, M., Oliveberg, M., and Marklund, S. L. (2006) *Brain* **129,** 451–464
35. Deng, H. X., Shi, Y., Furukawa, Y., Zhai, H., Fu, R., Liu, E., Gorrie, G. H., Khan, M. S., Hung, W. Y., Bigio, E. H., Lukas, T., Dal Canto, M. C., O'Halloran, T. V., and Siddique, T. (2006) *Proc. Natl. Acad. Sci. U. S. A.* **103,** 7142–7147
36. Getzoff, E. D., Tainer, J. A., Stempien, M. M., Bell, G. I., and Hallewell, R. A. (1989) *Proteins* **5,** 322–336
37. Briggs, R. G., and Fee, J. A. (1978) *Biochim. Biophys. Acta* **537,** 86–99
38. McRee, D. E., Redford, S. M., Getzoff, E. D., Lepock, J. R., Hallewell, R. A., and Tainer, J. A. (1990) *J. Biol. Chem.* **265,** 14234–14241
39. Lepock, J. R., Frey, H. E., and Hallewell, R. A. (1990) *J. Biol. Chem.* **265,** 21612–21618
40. Ripps, M. E., Huntley, G. W., Hof, P. R., Morrison, J. H., and Gordon, J. W. (1995) *Proc. Natl. Acad. Sci. U. S. A.* **92,** 689–693
41. Kabashi, E., Agar, J. N., Taylor, D. M., Minotti, S., and Durham, H. D. (2004) *J. Neurochem.* **89,** 1325–1335
42. Cheroni, C., Peviani, M., Cascio, P., Debiasi, S., Monti, C., and Bendotti, C. (2005) *Neurobiol. Dis.* **18,** 509–522
43. Di Noto, L., Whitson, L. J., Cao, X., Hart, P. J., and Levine, R. L. (2005) *J. Biol. Chem.* **280,** 39907–39913
44. Kabuta, T., Suzuki, Y., and Wada, K. (2006) *J. Biol. Chem.* **281,** 30524–30533
45. Lee, J. P., Gerin, C., Bindokas, V. P., Miller, R., Ghadge, G., and Roos, R. P. (2002) *J. Neurochem.* **82,** 1229–1238
46. Matsumoto, G., Stojanovic, A., Holmberg, C. I., Kim, S., and Morimoto, R. I. (2005) *J. Cell Biol.* **171,** 75–85
47. Arrasate, M., Mitra, S., Schweitzer, E. S., Segal, M. R., and Finkbeiner, S. (2004) *Nature* **431,** 805–810
48. Saudou, F., Finkbeiner, S., Devys, D., and Greenberg, M. E. (1998) *Cell* **95,** 55–66

ELSEVIER

Neurobiology of Disease

www.elsevier.com/locate/ynbdi
Neurobiology of Disease 25 (2007) 331–341

Dorfin-CHIP chimeric proteins potently ubiquitylate and degrade familial ALS-related mutant SOD1 proteins and reduce their cellular toxicity

Shinsuke Ishigaki,[a,b] Jun-ichi Niwa,[a] Shin-ichi Yamada,[a] Miho Takahashi,[a] Takashi Ito,[a] Jun Sone,[a] Manabu Doyu,[a] Fumihiko Urano,[b,c] and Gen Sobue[a,*]

[a]*Department of Neurology, Nagoya University Graduate School of Medicine, Nagoya 466-8500, Japan*
[b]*Program in Gene Function and Expression, University of Massachusetts Medical School, Worcester, MA 01605, USA*
[c]*Program in Molecular Medicine, University of Massachusetts Medical School, Worcester, MA 01605, USA*

Received 19 May 2006; revised 8 September 2006; accepted 22 September 2006
Available online 6 December 2006

The ubiquitin–proteasome system (UPS) is involved in the pathogenetic mechanisms of neurodegenerative disorders, including amyotrophic lateral sclerosis (ALS). Dorfin is a ubiquitin ligase (E3) that degrades mutant SOD1 proteins, which are responsible for familial ALS. Although Dorfin has potential as an anti-ALS molecule, its life in cells is short. To improve its stability and enhance its E3 activity, we developed chimeric proteins containing the substrate-binding hydrophobic portion of Dorfin and the U-box domain of the carboxyl terminus of Hsc70-interacting protein (CHIP), which has strong E3 activity through the U-box domain. All the Dorfin-CHIP chimeric proteins were more stable in cells than was wild-type Dorfin ($Dorfin^{WT}$). One of the Dorfin-CHIP chimeric proteins, $Dorfin\text{-}CHIP^{L}$, ubiquitylated mutant SOD1 more effectively than did $Dorfin^{WT}$ and CHIP *in vivo*, and degraded mutant SOD1 protein more rapidly than $Dorfin^{WT}$ does. Furthermore, $Dorfin\text{-}CHIP^{L}$ rescued neuronal cells from mutant SOD1-associated toxicity and reduced the aggresome formation induced by mutant SOD1 more effectively than did $Dorfin^{WT}$.

Keywords: Dorfin; ALS; SOD1; CHIP; Neurodegeneration; Ubiquitin–proteasome system

Amyotrophic lateral sclerosis (ALS), one of the most common neurodegenerative disorders, is characterized by selective motor neuron degeneration in the spinal cord, brainstem, and cortex. About 10% of ALS cases are familial; of these, 10%–20% are caused by Cu/Zn superoxide dismutase (SOD1) gene mutations (Rosen et al., 1993; Cudkowicz et al., 1997). However, the precise mechanism that causes motor neuron death in ALS is still unknown, although many have been proposed: oxidative toxicity, glutamate receptor abnormality, ubiquitin proteasome dysfunction, inflammatory and cytokine activation, neurotrophic factor deficiency, mitochondrial damage, cytoskeletal abnormalities, and activation of the apoptosis pathway (Julien, 2001; Rowland and Shneider, 2001).

Misfolded protein accumulation, one probable cause of neurodegenerative disorders, including ALS, can cause the deterioration of various cellular functions, leading to neuronal cell death (Julien, 2001; Ciechanover and Brundin, 2003). Recent findings indicate that the ubiquitin–proteasome system (UPS), a cellular function that recognizes and catalyzes misfolded or impaired cellular proteins (Jungmann et al., 1993; Lee et al., 1996; Bercovich et al., 1997), is involved in the pathogenesis of various neurodegenerative diseases, among them ALS, Parkinson's disease (PD), Alzheimer's disease, polyglutamine disease, and prion disease (Alves-Rodrigues et al., 1998; Sherman and Goldberg, 2001; Ciechanover and Brundin, 2003). The ubiquitin ligase (E3), a key molecule for the UPS, can specifically recognize misfolded substrates and convey them to proteasomal degradation (Scheffner et al., 1995; Glickman and Ciechanover, 2002; Tanaka et al., 2004).

Dorfin, an E3 protein, contains an in-between-ring-finger (RING-IBR) domain at its N-terminus. The C-terminus of Dorfin can recognize mutant SOD1 proteins, which cause familial ALS (Niwa et al., 2001; Ishigaki et al., 2002b; Niwa et al., 2002). In cultured cells, Dorfin colocalized with aggresomes and ubiquitin-positive inclusions, which are pathological hallmarks of neurodegenerative diseases (Hishikawa et al., 2003; Ito et al., 2003). Dorfin also interacted with VCP/p97 in ubiquitin-positive inclusions in

Abbreviations: ALS, amyotrophic lateral sclerosis; CFTR, cystic fibrosis transmembrane conductance regulator; CHIP, carboxyl terminus of Hsc70-interacting protein; DMEM, Dulbecco's modified Eagle's medium; E3, ubiquitin ligase; FCS, fetal calf serum; IP, immunoprecipitation; LB, Lewy body; PD, Parkinson's disease; RING-IBR, in-between-ring-finger; SCF, Skp1-Cullin-F box complex; SDS-PAGE, sodium dodecyl sulfate-polyacrylamide gel electrophoresis; SOD1, Cu/Zn super oxide dismutase; UPS, ubiquitin–proteasome system.

* Corresponding author. Fax: +81 52 744 2384.
E-mail address: sobueg@med.nagoya-u.ac.jp (G. Sobue).
Available online on ScienceDirect (www.sciencedirect.com).

0969-9961/$ - see front matter © 2006 Elsevier Inc. All rights reserved.
doi:10.1016/j.nbd.2006.09.017

ALS and PD (Ishigaki et al., 2004). Moreover, formation of this complex was found to be necessary for the E3 activity of Dorfin against mutant SOD1. These findings suggest that Dorfin is involved in the quality-control system for the abnormal proteins that accumulate in the affected neurons in neurodegenerative disorders.

Dorfin degrades mutant SOD1s and attenuates mutant SOD1-associated toxicity in cultured cells (Niwa et al., 2002). However, in Dorfin/mutant SOD1 double transgenic mice, we found only a modest beneficial effect on mutant SOD1-induced survival and motor dysfunction (unpublished data). These findings, combined with the short half-life of Dorfin protein, led us to hypothesize that the limiting effect of the Dorfin transgene may be a consequence of autodegradation of Dorfin, since Dorfin can execute autoubiquitilation *in vivo* (Niwa et al., 2001).

Carboxyl terminus of Hsc70-interacting protein (CHIP) is also an E3 protein; it has a TPR domain in the N terminus and a U-box domain in the C terminus. The U-box domain of CHIP is responsible for its strong E3 activity, whereas the TPR domain recruits heat shock proteins harboring misfolded client proteins such as cystic fibrosis transmembrane conductance regulator (CFTR), denatured luciferase, and tau (Meacham et al., 2001; Murata et al., 2001, 2003; Hatakeyama et al., 2004; Shimura et al., 2004).

To prolong the protein lifetime of Dorfin and thereby obtain more potent ubiquitylation and degradation activity against mutant SOD1s than is provided by Dorfin or CHIP alone, we generated chimeric proteins containing the substrate-binding domain of Dorfin and the UPR domain of CHIP substitute for RING/IBR of Dorfin. We developed 12 candidate constructs that encode Dorfin-CHIP chimeric proteins and analyzed them for their E3 activities and degradation abilities against mutant SOD1 protein in cultured cells.

Experimental procedures

Plasmids and antibodies

We designed constructs expressing Dorfin-CHIP chimeric protein. In these constructs, different-length fragments of the C-terminus portion of Dorfin, including the hydrophobic substrate-binding domain (amino acids 333–838, 333–700, and 333–454) and the C-terminus UPR domain of CHIP with amino acids 128–303 or without amino acids 201–303, a charged region was fused in various combinations as shown in Fig. 2C. Briefly, Dorfin-CHIP$^{A, B, C, G, H, I}$ had the C-terminus portion of Dorfin in their N-terminus and the U-box of CHIP in their C-terminus; Dorfin-CHIP$^{D, E, F, J, K, L}$ had the U-box of CHIP in their N-terminus and the C-terminus portion of Dorfin in their C-terminus.

We prepared a pCMV2/FLAG-Dorfin-CHIP chimeric vector (Dorfin-CHIP) by polymerase chain reaction (PCR) using the appropriate design of PCR primers with restriction sites (*Cla*I, *Kpn*I, and *XBa*I or *Eco*RI, *Cla*I, and *Kpn*I). The PCR products were digested and inserted into the *Cla*I–*Kpn*I site in pCMV2 vector (Sigma, St. Louis, MO). These vectors have been described previously: pFLAG-Dorfin^{WT} (Dorfin^{WT}), FLAG-Dorfin$^{C132S/C135S}$ (Dorfin$^{C132S/C135S}$), pFLAG-CHIP (CHIP), pFLAG-Mock (Mock), pcDNA3.1/Myc-SOD1^{WT} (SOD1^{WT}), pcDNA3.1/Myc-SOD1^{G93A} (SOD1^{G93A}), pcDNA3.1/Myc-SOD1^{G85R} (SOD1^{G85R}), pcDNA3.1/Myc-SOD1^{H46R} (SOD1^{H46R}), pcDNA3.1/Myc-SOD1^{G37R} (SOD1^{G37R}), pEGFP/SOD1^{WT} (SOD1^{WT}-GFP), and pEGFP/SOD1^{G85R} (SOD1^{G85R}-GFP) (Ishigaki et al., 2004). We used monoclonal anti-FLAG antibody (M2; Sigma), monoclonal anti-Myc antibody (9E10; Santa Cruz Biotechnology, Santa Cruz, CA), monoclonal anti-HA antibody (12CA5; Roche, Basel, Switzerland), and polyclonal anti-SOD1 (SOD-100; Stressgen, San Diego, CA).

Cell culture and transfection

We grew HEK293 cells and neuro2a (N2a) cells in Dulbecco's modified Eagle's medium (DMEM) containing 10% fetal calf serum (FCS), 5 U/ml penicillin, and 50 μg/ml streptomycin. At subconfluence, we transfected these cells with the indicated plasmids, using Effectene reagent (Qiagen, Valencia, CA) for HEK293 cells and Lipofectamine 2000 (Invitrogen, Carlsbad, CA) for N2a cells. After overnight posttransfection, we treated the cells with 1 μM MG132 (Z-Leu-Leu-Leu-al; Sigma) for 16 h to inhibit cellular proteasome activity. We analyzed the cells 24–48 h after transfection. To differentiate N2a cells, cells were treated for 48 h with 15 μM of retinoic acid in 2% serum medium.

Immunological analysis

At 24–48 h after transfection, we lysed cells (4×10^5 in 6-cm dishes) with 500 μl of lysis buffer consisting of 50 mM Tris–HCl, 150 mM NaCl, 1% Nonidet P-40, and 1 mM ethylenediaminetetraacetic acid (EDTA), as well as a protease inhibitor cocktail (Complete Mini, Roche). The lysate was then centrifuged at $10{,}000 \times g$ for 10 min at 4°C to remove debris. We used a 10% volume of the supernatants as the lysate for SDS-PAGE. When immunoprecipitated, the supernatants were precleared with protein A/G agarose (Santa-Cruz). A specific antibody, either anti-FLAG (M2) or anti-Myc (9E10), was then added. We incubated the immune complexes, first at 4°C with rotation and with protein A/G agarose (Roche) for 3 h, after which they were collected by centrifugation and washed four times with the lysis buffer. For protein analysis, immune complexes were dissociated by heating in SDS-PAGE sample buffer and loaded onto SDS-PAGE. We separated the samples by SDS-PAGE (15% gel or 5%–20% gradient gel) and transferred them onto polyvinylidene difluoride membranes. We then immunoblotted samples with specific antibodies.

Immunohistochemistry

We fixed differentiated N2a cells grown in plastic dishes in 4% paraformaldehyde in PBS for 15 min. The cells were then blocked for 30 min with 5% (vol/vol) normal goat serum in PBS, incubated overnight at 4°C with anti-FLAG antibody (M2), washed with PBS, and incubated for 30 min with Alexa 496 nm anti-mouse antibodies (Molecular Probes, Eugene, OR). We mounted the cells on slides and obtained images using a fluorescence microscope (IX71; Olympus, Tokyo, Japan) equipped with a cooled charge-coupled device camera (DP70; Olympus). Photographs were taken using DP Controller software (Olympus).

Analysis of protein stability

We assayed the stability of proteins by pulse-chase analysis using [^{35}S] followed by immunoprecipitation. Metabolic labeling was performed as described previously (Yoshida et al., 2003). Briefly, in the pulse-chase analysis of Dorfin proteins, HEK293 cells in 6-cm dishes were transiently transfected with 1 μg of

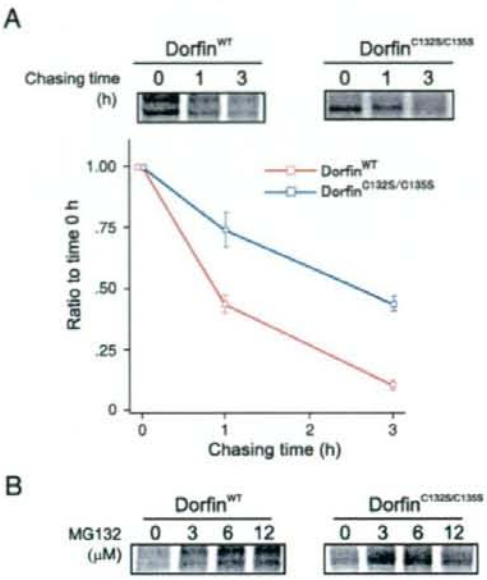

Fig. 1. Pulse-chase analysis of Dorfin^{WT} and Dorfin$^{C132S/C135S}$. (A) Dorfin^{WT} or Dorfin$^{C132S/C135S}$ was overexpressed in HEK293 cells. After overnight incubation, [^{35}S]-labeled Met/Cys pulse-chase analysis was performed. Cells were harvested and analyzed at 0, 1, or 3 h after labeling and immunoprecipitation by anti-FLAG antibody (upper panels). To determine serial changes in the amount of Dorfin^{WT} or Dorfin$^{C132S/C135S}$, four independent experiments were performed and the amounts of Dorfin^{WT} and Dorfin$^{C132S/C135S}$ were plotted. The differences between the amounts of Dorfin^{WT} and Dorfin$^{C132S/C135S}$ were significant at 1 h ($p<0.01$) and 3 h after labeling ($p<0.001$) (lower panels). Values are the means ± SE, $n=4$. Statistics were done using an unpaired t-test. (B) Cells overexpressing Dorfin^{WT} or Dorfin$^{C132S/C135S}$ were treated with different concentrations of MG132 for 3 h after labeling.

FLAG-Dorfin^{WT} or FLAG-Dorfin$^{C132S/C135S}$. In pulse-chase experiments using SOD1^{G85R}, N2a cells in 6-cm dishes were transiently transfected with 1 μg of SOD1^{G85R}-Myc or SOD1^{G93A}-Myc and FLAG-Mock, FLAG-Dorfin, or FLAG-Dorfin-CHIP^{L}. FLAG-Mock was used as a negative control. After starving the cells for 60 min in methionine- and cysteine-free DMEM with 10% FCS, we labeled them for 60 min with 150 μCi/ml of Pro-Mix L-[^{35}S] *in vitro* cell-labeling mix (Amersham Biosciences). Cells were chased for different lengths of time at 37°C. In experiments with proteasomal inhibition, we added different amounts of MG132 in medium during the chase period. We performed immunoprecipitation using protein A/G agarose, mouse monoclonal anti-FLAG (M2), and anti-Myc (9E10). The intensity of the bands was quantified by ImageGauge software (Fuji Film, Tokyo, Japan).

MTS assay

We transfected N2a cells (5000 cells per well) in 96-well collagen-coated plates with 0.15 μg of SOD1^{G85R}-GFP and 0.05 μg of Dorfin, CHIP, Dorfin-CHIP^{L}, or pCMV2 vector (Mock) using Effecten reagent (Qiagen). Then we performed 3-(4,5-dimethylthiazol-2-yl)-5-(3-carboxymethoxyphenyl)-2-(4-sulfophenyl)-2*H*-tetrazolium inner salt (MTS) assays using Cell Titer 96 (Promega) at 48 h after incubation. This procedure has previously been described (Ishigaki et al., 2002a).

Aggregation assay

We transfected N2a cells in 6-cm dishes with 1.0 μg of SOD1^{G85R}-GFP and 1.0 μg of FLAG-Mock, FLAG-Dorfin, FLAG-CHIP, or FLAG-Dorfin-CHIP^{L}. After overnight incubation, we changed the medium to 2% FCS containing medium with 15 μM retinoic acid (RA) for differentiation. In the MG132 (+) group, 1 μM of MG132 was added after 24 h of differentiation stimuli. After 48 h of differentiation stimuli, we examined the cells in their living condition by fluorescence microscopy. The transfection ratio was equivalent (75%) among all groups. Visually observable macro aggregation-harboring cells were counted as "aggregation positive" cells (Fig. 7C). All cells were counted in fields selected at random from the four different quadrants of the culture dish. Counting was done by an investigator who was blind to the experimental condition.

Results

Dorfin degradation by the UPS in vivo

We analyzed the degradation speed of FLAG-Dorfin by the pulse-chase method using [^{35}S] labeling, finding that more than half of wild-type Dorfin (Dorfin^{WT}) was degraded within 1 h (Fig. 1A). This degradation was dose-dependently inhibited by MG132, a proteasome inhibitor (Fig. 1B). On the other hand, the RING mutant form of Dorfin (Dorfin$^{C132S/C135S}$), which lacks E3 activity (Ishigaki et al., 2004), degraded significantly more slowly than did Dorfin^{WT} (Fig. 1A and Table 1). As shown in Fig. 1A, Dorfin^{WT} showed two bands, whereas Dorfin$^{C132S/C135S}$ had a single band. This was also seen in our previous study (Ishigaki et al., 2004) and may represent posttranslational modification.

Construction of Dorfin-CHIP chimeric proteins

It is known that the C-terminus portion of Dorfin can bind to substrates such as mutant SOD1 proteins or Synphilin-1 (Niwa et al., 2002; Ito et al., 2003). We attempted to identify the domain of Dorfin that interacts with substrates. Although there was no obvious known motif in the C-terminus of Dorfin (amino acids 333–838), its first quarter contained rich hydrophobic amino acids (amino acids 333–454) (Fig. 2A). Immunoprecipitation analysis revealed that the hydrophobic region of Dorfin (amino acids 333–454) was able to bind to SOD1^{G85R}, indicating that this hydrophobic region is responsible for recruiting mutant SOD1 in Dorfin protein (Fig. 2B).

To establish more effective and more stable E3 ubiquitin ligase molecules that can recognize and degrade mutant SOD1s, we

Table 1
Serial changes in the amounts of Dorfin^{WT}, Dorfin$^{C132S/C135S}$, and Dorfin-CHIP^{L}

	0 h (%)	1 h (%)	3 h (%)
Dorfin^{WT}	100	43.7±7.0	10.3±4.4
Dorfin$^{C132S/C135S}$	100	73.9±13.8	43.7±1.9
Dorfin-CHIP^{L}	100	89.0±5.7	47.5±5.3

Values are the mean and SD of four independent experiments.

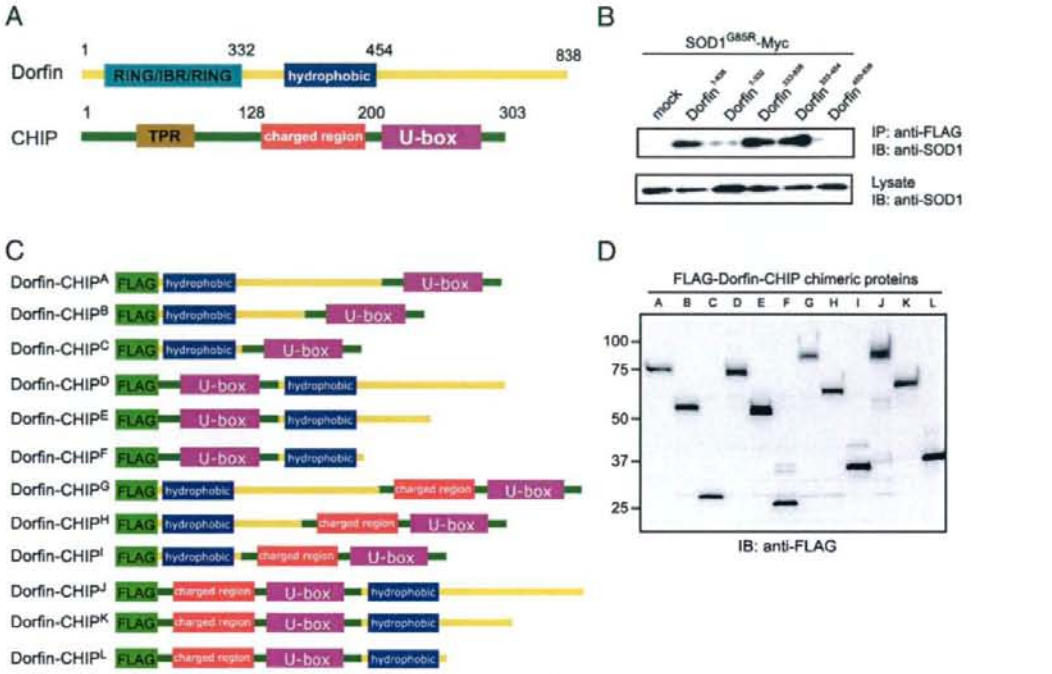

Fig. 2. Construction of Dorfin-CHIP chimeric proteins. (A) Dorfin has a RING/IBR domain in its N-terminus and a substrate-binding portion in the C-terminus. CHIP contains a TPR domain that binds to heat-shock proteins at the N-terminus; its C-terminal U-box domain has strong E3 ubiquitin ligase activity. (B) SOD1^{G85R}-Myc and FLAG-Dorfin derivatives were overexpressed in HEK 293 cells. Cell lysates were immunoprecipitated with anti-myc antibody. Immunoblotting showed that FLAG-Dorfin derivatives containing Dorfin$^{333-454}$ bound to SOD1^{G85R}-Myc, indicating that the hydrophobic region of Dorfin (Dorfin$^{333-454}$) is essential for interaction with mutant SOD1 *in vivo*. (C) Scheme of engineered Dorfin-CHIP chimeric proteins. Three different lengths of C-terminal Dorfin containing the hydrophobic region of Dorfin (Dorfin$^{333-454}$) and the U-box domain of CHIP with or without the charged region were fused. (D) Dorfin-CHIP chimeric proteins were overexpressed in HEK293 cells. Harvested cells were lysed and analyzed by immunoblotting using anti-FLAG antibody.

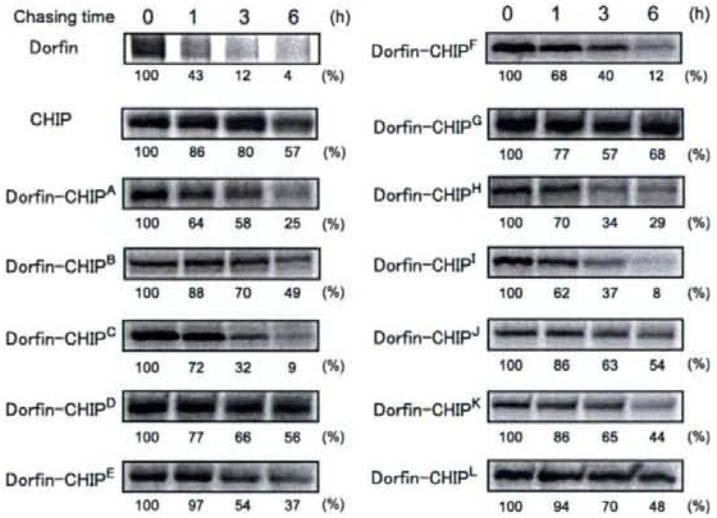

Fig. 3. The stability of Dorfin-CHIP chimeric proteins. Pulse-chase analysis using [^{35}S]-Met/Cys was performed. Dorfin, CHIP, and all the Dorfin-CHIP chimeric proteins were overexpressed in HEK293 cells and labeled with [^{35}S]-Met/Cys. Immunoprecipitation using anti-FLAG antibody and SOD-PAGE analysis revealed the degradation speed of FLAG-Dorfin-CHIP chimeric proteins. The amount of each Dorfin-CHIP chimeric protein was measured by quantifying the band using ImageGauge software.

designed Dorfin-CHIP chimeric proteins containing both the hydrophobic substrate-binding domain of Dorfin and the U-box domain of CHIP, which has strong E3 activity (Fig. 2C). We verified that all of the 12 candidate chimeric proteins were expressed in HEK293 cells (Fig. 2D).

Expression of Dorfin-CHIP chimeric proteins in cells

The half lives of all the Dorfin-CHIP chimeric proteins were more than 1 h. In some of these proteins, such as Dorfin-CHIP$^{D, G, J}$, and ^{L}, moderate amounts of protein still remained at 6 h after labeling, indicating that they were degraded much more slowly than was Dorfin^{WT} (Fig. 3). Repetitive experiments using Dorfin-CHIP^{L} yielded a significant difference between the amount of Dorfin^{WT} and Dorfin-CHIP^{L} at 1 h and 3 h (Table 1).

E3 activity of Dorfin-CHIP chimeric proteins against mutant SOD1

Immunoprecipitation analysis demonstrated that Dorfin and CHIP bound to mutant SOD1^{G85R} in equivalent amounts and that all of the Dorfin-CHIP chimeric proteins interacted with mutant SOD1^{G85R} *in vivo*. Dorfin-CHIP$^{A, D, E, F, J, K}$, and ^{L} bound to the same or greater amounts of SOD1^{G85R} than did Dorfin, whereas Dorfin-CHIP$^{B, C, G, H}$, and ^{I} did not (Fig. 4A, upper panel). None of the Dorfin-CHIP chimeric proteins bound to SOD1^{WT} *in vivo*

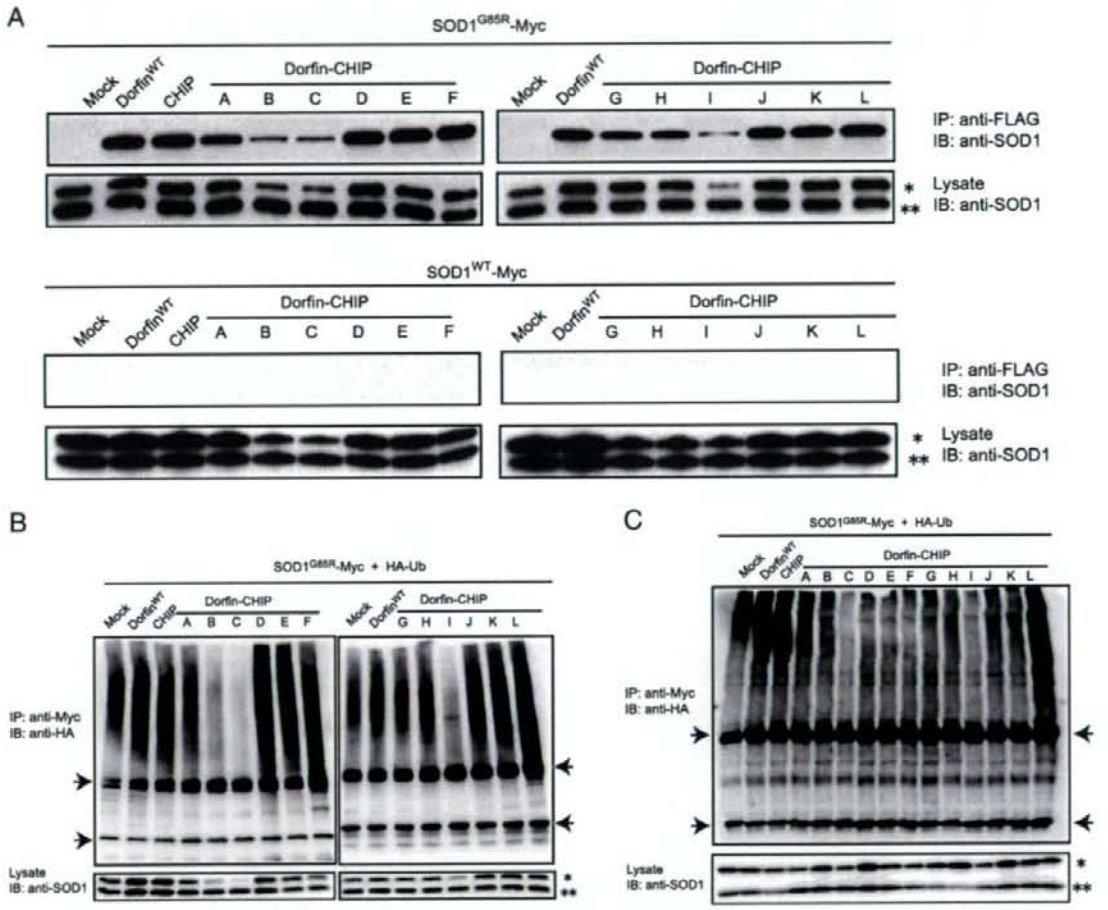

Fig. 4. The E3 activity of Dorfin-CHIP chimeric proteins on mutant SOD1 *in vivo*. (A) *In vivo* binding assay with both wild-type and mutant SOD1s. SOD1^{G85R}- or SOD1^{WT}-Myc and FLAG derivatives of Dorfin-CHIP chimeric proteins were coexpressed in HEK293 cells. Immunoprecipitation was done using anti-Myc antibody. Immunoblotting with anti-FLAG antibody revealed that all the Dorfin-CHIP chimeric proteins bound *in vivo* to SOD1^{G85R}-Myc but not to SOD1^{WT}-Myc. Single and double asterisks indicate overexpressed human SOD1s and mouse endogenous SOD1, respectively. (B) *In vivo* ubiquitylation assay in HEK293 cells. SOD1^{G85R}-Myc, HA-Ub, and FLAG derivatives of Dorfin-CHIP chimeric proteins were coexpressed in HEK293 cells. Immunoblotting with anti-HA antibody demonstrated the ubiquitylation level of SOD1^{G85R}-Myc by FLAG derivatives of Dorfin-CHIP chimeric proteins *in vivo*. Arrows indicate IgG light and heavy chains. Single and double asterisks indicate overexpressed SOD1 and mouse endogenous SOD1, respectively. (C) *In vivo* ubiquitylation assay in N2a cells. SOD1^{G85R}-Myc, HA-Ub, and FLAG derivatives of Dorfin-CHIP chimeric proteins were coexpressed in N2a cells. Arrows indicate IgG light and heavy chains. Single and double asterisks indicate overexpressed human SOD1s and mouse endogenous SOD1, respectively.

(Fig. 4A, lower panel). Some Dorfin-CHIP chimeric proteins, such as Dorfin-CHIP$^{B, C}$, and ^{I}, had lower amounts of both SOD1^{WT} and SOD1^{G85R} in the lysates. We performed quantitative RT-PCR using specific primers for SOD1-Myc, finding that coexpression of Dorfin-CHIP$^{B, C}$ or ^{I} suppressed the mRNA expression of overexpressed SOD1 gene (Supplementary Fig. 1). Considering the possibility that these Dorfin-CHIP chimeric proteins might have unpredicted toxicity for cells by affecting gene transcription via unknown mechanisms, we excluded them from further analysis. Other Dorfin-CHIP proteins did not affect SOD1-Myc gene expression, which validated the comparison among IPs and ubiquitylated mutant SOD1 in Figs. 4A–C.

To assess the effectiveness of the E3 activity of Dorfin-CHIP chimeric proteins, we did an *in-vivo* ubiquitylation analysis by coexpression of SOD1^{G85R}-Myc, HA-Ub, and Dorfin-CHIP chimeric proteins in HEK293 cells. We found that Dorfin and CHIP enhanced the ubiquitylation of SOD1^{G85R} protein and that the ubiquitylation levels of these two E3 ligases were almost equivalent. Moreover, Dorfin-CHIP$^{D, E, F, J, K}$, and ^{L} ubiquitylated SOD1^{G85R} more effectively than did Dorfin or CHIP (Fig. 4B).

Performing the same *in-vivo* ubiquitylation assay using N2a cells, we observed that the levels of ubiquitylation of SOD1^{G85R} by Dorfin and CHIP were equivalent, as they were in HEK293 cells. Among Dorfin-CHIP chimeric proteins, only Dorfin-CHIP^{L}

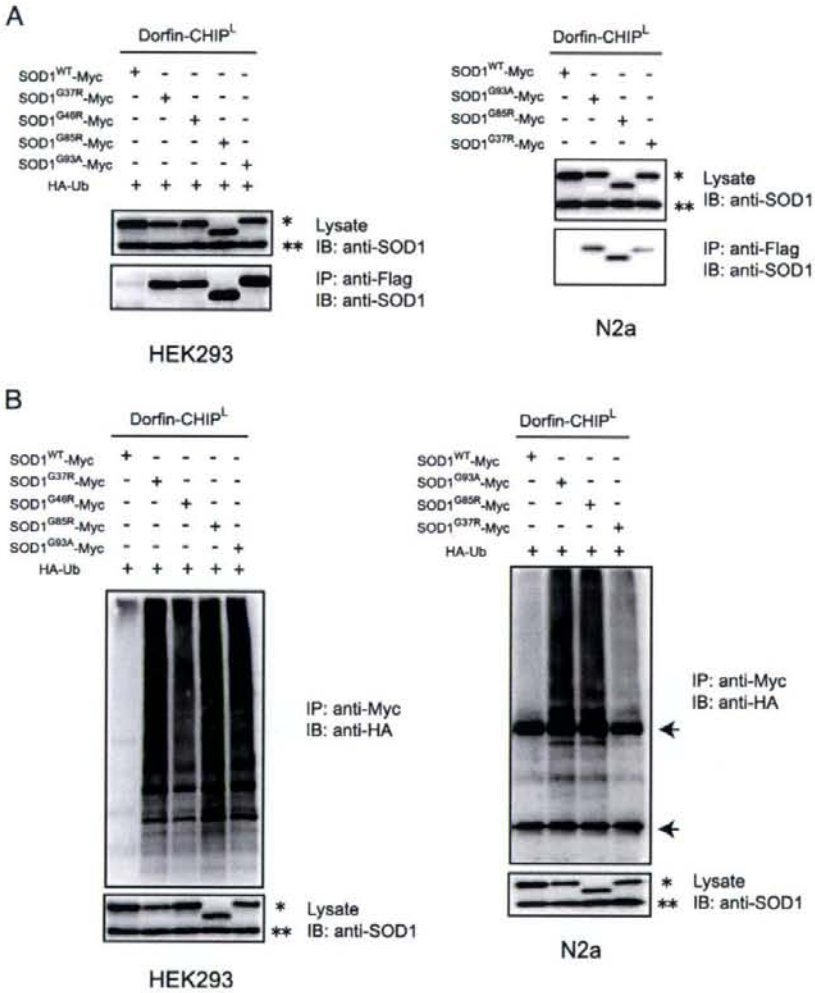

Fig. 5. Dorfin-CHIP^{L} specifically ubiquitylates mutant SOD1s *in vivo*. (A) *In vivo* binding assay with various mutant SOD1s. SOD1^{WT}-Myc, SOD1^{G93A}-Myc, SOD1^{G85R}-Myc, SOD1^{H46R}-Myc or SOD1^{G37R}-Myc, and FLAG-Dorfin-CHIP^{L} were coexpressed in HEK293 (left) and N2a cells (right). Immunoprecipitation was done using anti-Myc antibody. Immunoblotting with anti-FLAG antibody showed that both chimeric proteins specifically bound to mutant SOD1s *in vivo*. Single and double asterisks indicate overexpressed SOD1 and mouse endogenous SOD1, respectively. (B) *In vivo* ubiquitylation assay. SOD1^{WT}-Myc, SOD1^{G93A}-Myc, SOD1^{G85R}-Myc, SOD1^{H46R}-Myc or SOD1^{G37R}-Myc, as well as FLAG-Dorfin-CHIP^{L} and HA-Ub, was coexpressed in HEK293 (left) and N2a cells (right). Immunoblotting with anti-HA antibody showed the specific ubiquitylation of mutant SOD1-Myc by FLAG-Dorfin-CHIP^{L} *in vivo*. Arrows indicate IgG light and heavy chains. Single and double asterisks indicate overexpressed human SOD1s and mouse endogenous SOD1, respectively.

ubiquitylated SOD1^{G85R} more effectively than did Dorfin or CHIP, while Dorfin-CHIP$^{D, E, F, J}$, and ^{K} did not (Fig. 4C). Thus, Dorfin-CHIP^{L} was the most potent candidate of the chimeric proteins.

Ubiquitylation of mutant SOD1 by Dorfin-CHIP^{L}

Dorfin specifically ubiquitylated mutant SOD1 proteins, but not SOD1^{WT} protein (Niwa et al., 2002; Ishigaki et al., 2004). Similarly, Dorfin-CHIP^{L} interacted with SOD1^{G93A}, SOD1^{G85R}, SOD1^{H46R}, and SOD1^{G37R}, but not SOD1^{WT}, in HEK293 cells. This was confirmed in N2a cells (Fig. 5A). In both HEK293 and N2a cells, Dorfin-CHIP^{L} also ubiquitylated mutant SOD1 proteins but not SOD1^{WT} (Fig. 5B).

Degradation of mutant SOD1 by Dorfin-CHIP chimeric proteins

To assess the degradation activity of Dorfin-CHIP^{L} against mutant SOD1s, we performed the pulse-chase analysis on N2a

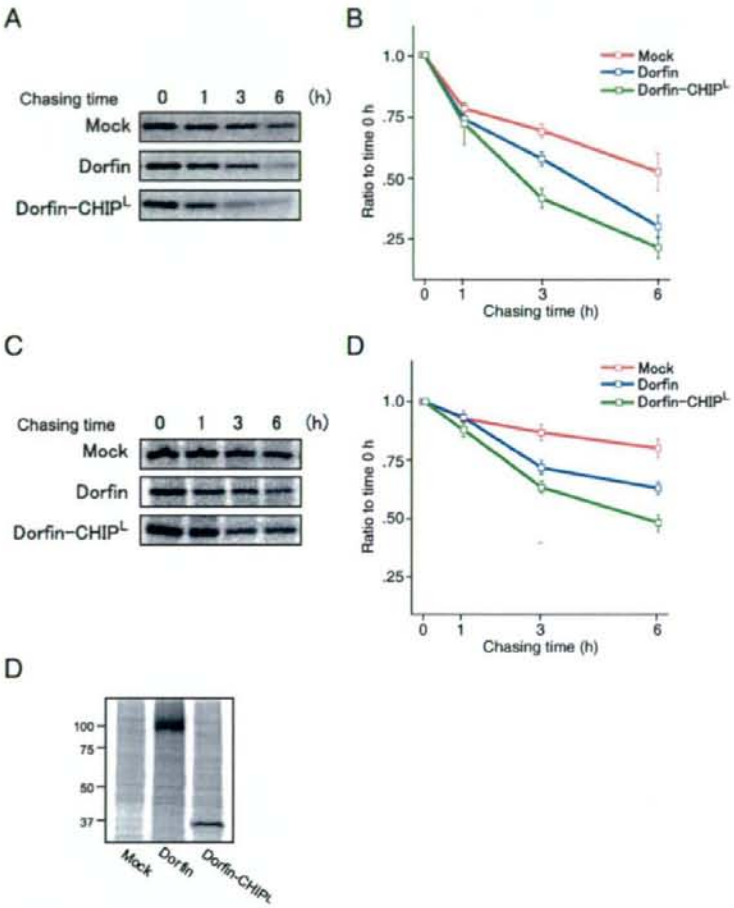

Fig. 6. Degradation of mutant SOD1 proteins with Dorfin-CHIP^{L}. (A) Pulse-chase analysis of SOD1^{G85R} with Dorfin-CHIP^{L}. N2a cells were coexpressed with SOD1^{G85R}-Myc and Mock, Dorfin, and Dorfin-CHIP^{L}. Pulse-chase experiments using [^{35}S]-Met/Cys were done. Immunoprecipitation using anti-Myc antibody and SOD-PAGE analysis revealed the degradation speed of SOD1^{G85R}-Myc. (B) Serial changes in the amount of SOD1^{G85R} coexpressed with Mock, Dorfin, or Dorfin-CHIP^{L}. Four independent experiments were performed and the amounts of SOD1^{G85R} were plotted. There were significant differences between Mock and Dorfin ($p<0.005$), Mock and Dorfin-CHIP^{L} ($p<0.005$), and Dorfin and Dorfin-CHIP^{L} ($p<0.05$) at 3 h, as well as between Mock and Dorfin ($p<0.05$), and Mock and Dorfin-CHIP^{L} ($p<0.05$) at 6 h after labeling. Values are the means ± SE, $n=4$. Statistical analysis was done by one-way ANOVA. (C) Pulse-chase analysis of SOD1^{G93A} with Dorfin-CHIP^{L}. N2a cells were coexpressed with SOD1^{G93A}-Myc and Mock, Dorfin, and Dorfin-CHIP^{L} as in panel A. (D) Serial changes in the amount of SOD1^{G93A} coexpressed with Mock, Dorfin, or Dorfin-CHIP^{L}. Four independent experiments were performed and the amounts of SOD1^{G93A} were plotted. There were significant differences between Mock and Dorfin ($p<0.05$) and Mock and Dorfin-CHIP^{L} ($p<0.01$) at 3 h, as well as between Mock and Dorfin ($p<0.05$), Mock and Dorfin-CHIP^{L} ($p<0.01$), and Dorfin and Dorfin-CHIP^{L} ($p<0.05$) at 6 h after labeling. Values are the means ± SE, $n=4$. Statistics were done by one-way ANOVA. (E) The equivalent protein expression levels of Dorfin and Dorfin-CHIP^{L}. Half of the volume of samples used in the pulse-chase analysis of panel C at 0 h was used for immunoprecipitation using anti-Flag M2 antibody. The following SOD-PAGE analysis revealed the amounts of Dorfin and Dorfin-CHIP^{L} in the experiment shown in panel C.

cells, using [^{35}S] labeled Met/Cys. The protein levels of SOD1^{G85R} and SOD1^{G93A} declined more rapidly with Dorfin coexpression. Dorfin-CHIP^{L} remarkably declined in both SOD1^{G85R} and SOD1^{G93A} (Figs. 6A, C). Dorfin and Dorfin-CHIP^{L} had similar expression levels at 0 h of this experiment (Fig. 6E). As compared to Mock, Dorfin showed significant declines of both SOD1^{G85R} at 3 h ($p<0.001$) and 6 h ($p<0.05$) after labeling, as shown in a previous study (Niwa et al., 2002). Dorfin-CHIP^{L} also significantly accelerated the decline of SOD1^{G85R} at 3 h ($p<0.001$) and 6 h ($p<0.05$) after labeling again as compared to Mock. At 3 h after labeling, a significant difference between Dorfin-CHIP^{L} and Dorfin was present with respect to SOD1^{G85R} degradation ($p<0.05$). As compared to Dorfin, Dorfin-CHIP^{L} also tended toward accelerated SOD1^{G85R} degradation at 6 h after labeling (Fig. 6B). Similarly, Dorfin showed significant declines of SOD1^{G93A} at 3 h ($p<0.05$) and 6 h ($p<0.05$) after labeling, and Dorfin-CHIP^{L} significantly accelerated the declines of SOD1^{G93A} at 3 h ($p<0.01$) and 6 h ($p<0.01$) after labeling as compared to Mock. A significant difference between Dorfin-CHIP^{L} and Dorfin was present at 6 h in SOD1^{G93A} degradation ($p<0.05$) (Fig. 6D).

Attenuation of the toxicity of mutant SOD1 and decrease in the formation of visible aggregations of mutant SOD1 in cultured neuronal culture cells

The ability of Dorfin-CHIP chimeric proteins to attenuate mutant SOD1-related toxicity was analyzed by MTS assay using N2a cells. The expression of SOD1^{G85R}, as compared to that of SOD1^{WT}, decreased the viability of cells. Overexpression of Dorfin reversed the toxic effect of SOD1^{G85R}, whereas overexpression of CHIP did not. Dorfin-CHIP^{L} had a significantly greater rescue effect on SOD1^{G85R}-related cell toxicity than did Dorfin (Fig. 7A). We also measured the cell viability of N2a cells overexpressing Mock, Dorfin, and Dorfin-CHIP^{L} with various amounts of constructs, and found no difference in toxicity among them (Supplementary Fig. 2).

A structure that Johnston et al. (1998) called aggresome is formed when the capacity of a cell to degrade misfolded proteins is exceeded. The accumulation of mutant SOD1 induces visible macroaggregation, which is considered to be 'aggresome' in N2a cells. We examined the subcellular localizations of Dorfin, CHIP, and Dorfin-CHIP^{L} by immunostaining N2a cells expressing SOD1^{G85R}-GFP. Dorfin was localized in aggresomes with substrate proteins, as in our previous studies. Dorfin-CHIP^{L} was also seen in aggresomes, whereas the staining of CHIP was diffusely observed in the cytosol (Fig. 7B). We counted these visible aggregations with or without MG132 treatment. Dorfin decreased the number of aggregation-containing cells, as has been reported (Niwa et al., 2002), but Dorfin-CHIP^{L} did so more effectively. These effects were inhibited by the treatment of MG132 (Fig. 7C).

Discussion

E3 proteins can specifically recognize and degrade accumulating aberrant proteins, which are deeply involved in the pathogenesis of neurodegenerative disorders, including ALS (Alves-Rodrigues et al., 1998; Sherman and Goldberg, 2001; Ciechanover and Brundin, 2003). For this reason, E3 proteins are candidate molecules for use in developing therapeutic technology for neurodegenerative diseases. Dorfin is the first E3 molecule that has been found specifically to ubiquitylate mutant SOD1 proteins as well as to attenuate mutant SOD-associated toxicity in cultured neuronal cells (Niwa et al., 2002).

NEDL1, a HECT type E3 ligase, has also been reported to be a mutant SOD1-specific E3 ligase and to interact with TRAPδ and dvl1 (Miyazaki et al., 2004). It has also been reported that ubiquitylation of mutant SOD1-associated complex was enhanced by CHIP and Hsp70 *in vivo* (Urushitani et al., 2004). CHIP ubiquitylated Hsp70-holding SOD1 complexes and degraded mutant SOD1, but did not directly interact with mutant SOD1 (Urushitani et al., 2004). Among these E3 molecules, Dorfin seems to be the most potentially beneficial E3 protein for use in ALS therapy since it is the only one that has been demonstrated to reverse mutant SOD1-associated toxicity (Niwa et al., 2002). Furthermore, Dorfin has been localized in various ubiquitin-positive inclusions such as Lewy bodies (LB) in PD, as well as LB-like inclusions in sporadic ALS and glial cell bodies in multiple-system atrophy. These findings indicate that Dorfin may be involved in the pathogenesis of a broad spectrum of neurodegenerative disorders other than familial ALS (Hishikawa et al., 2003; Ito et al., 2003; Ishigaki et al., 2004).

The half-life of Dorfin^{WT} is, however, less than 1 h (Fig. 1, Table 1). The amount of Dorfin is increased in the presence of MG132, a proteasome inhibitor, indicating that Dorfin is immediately degraded in the UPS. Since the nonfunctional RING mutant form of Dorfin, Dorfin$^{C132S/C135S}$, degraded more slowly than did Dorfin^{WT}, Dorfin seemed to be degraded by auto-ubiquitylation. The degradation of Dorfin$^{C132S/C135S}$ is also inhibited by MG132, suggesting that it is degraded by endogenous Dorfin or other E3s. This immediate degradation of Dorfin is a serious problem for its therapeutic application against neurodegenerative diseases.

Several reports have shown that engineered chimera E3s are able to degrade certain substrates with high efficiency. Protac, a chimeric protein-targeting molecule, was designed to target methionine aminopeptidase-2 to Skp1-Cullin-F box complex (SCF) ubiquitin ligase complex for ubiquitylation and degradation (Sakamoto et al.,

Fig. 7. Dorfin-CHIP chimeric proteins can attenuate toxicity induced by mutant SOD1 and decrease the formation of visible aggregation of mutant SOD1 in N2a cells. (A) N2a cells were grown in 96 collagen-coated wells (5000 cells per well) and transfected with 0.15 μg of SOD1^{WT} and 0.05 μg of Mock or 0.15 μg of SOD1^{G85R} and 0.05 μg of Mock, Dorfin, CHIP, or Dorfin-CHIP^{L}. After the medium was changed, MTS assays were done at 48 h of incubation. Viability was measured as the level of absorbance (490 nm). Values are the means ± SE, $n=6$. Statistics were carried out by one-way ANOVA. There were significant differences between SOD1^{G85R}-expressing cells coexpressed with Mock and SOD1^{G85R}-expressing cells coexpressed with Dorfin ($p<0.001$), as well as between SOD1^{G85R}-expressing cells coexpressed with Dorfin and SOD1^{G85R}-expressing cells coexpressed with Dorfin-CHIP^{L} ($p<0.001$). (B) N2a cells were transiently expressed with SOD1^{G85R}-GFP and Mock, Dorfin, CHIP, or Dorfin-CHIP^{L}. Immunostaining with anti-FLAG antibody revealed that Dorfin, CHIP, and Dorfin-CHIP^{L} were localized with SOD1^{G85R}-GFP in macroaggresomes (arrows). Scale bar=20 μm (C) The visible macroaggregations in N2a cells expressing both SOD1^{G85R}-GFP and Mock, Dorfin, CHIP, or Dorfin-CHIP^{L} with or without MG132 treatment were counted and the ratio of cells with aggregations to those with GFP signals was calculated. Values are the means ± SE, $n=4$. Statistics were done by one-way ANOVA. *$p<0.01$ denotes a significant difference between cells with Mock and Dorfin or Dorfin-CHIP^{L}. **$p<0.05$ denotes a significant difference between cells with Dorfin and Dorfin-CHIP^{L}.

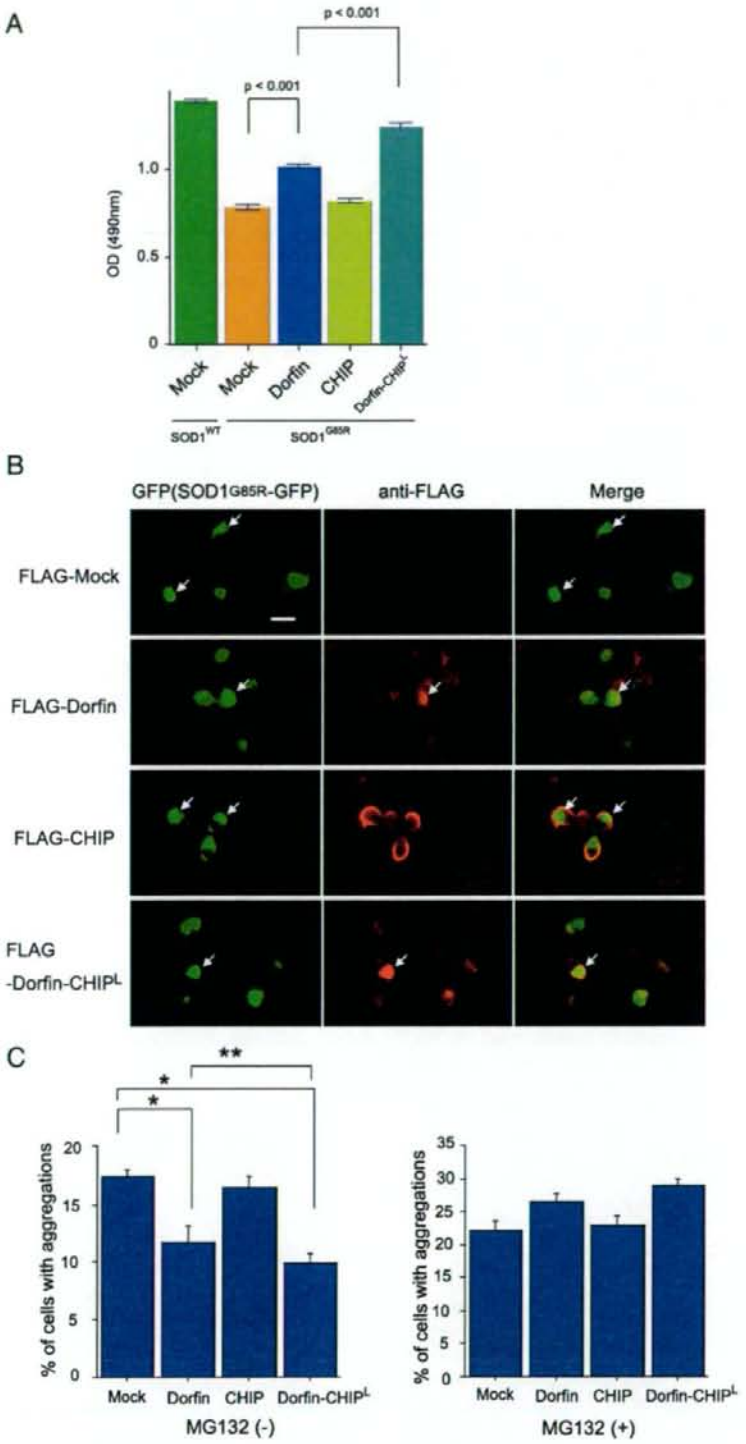
A
p < 0.001
p < 0.001
OD (490nm)
1.0
0.5
0
Mock
Mock
Dorfin
CHIP
Dorfin-CHIP^L
SOD1^WT
SOD1^G85R
B
GFP(SOD1G85R-GFP)
anti-FLAG
Merge
FLAG-Mock
FLAG-Dorfin
FLAG-CHIP
FLAG
-Dorfin-CHIP^L
C
**
*
*
% of cells with aggregations
20
15
10
5
0
Mock
Dorfin
CHIP
Dorfin-CHIP^L
MG132 (-)
% of cells with aggregations
35
30
25
20
15
10
5
0
Mock
Dorfin
CHIP
Dorfin-CHIP^L
MG132 (+)

2001, 2003). Oyake et al. (2002) developed double RING ubiquitin ligases containing the RING finger domains of both BRCA and BARD1 linked to a substrate recognition site PCNA. Recently, Hatakeyama et al. developed a fusion protein composed of Max, which forms a heterodimer with c-Myc, and the U-box of CHIP. This fusion protein physically interacted with c-Myc and promoted the ubiquitylation of c-Myc. It also reduced the stability of c-Myc, resulting in the suppression of transcriptional activity dependent on c-Myc and the inhibition of tumorogenesis (Hatakeyama et al., 2005). This indicated that the U-box portion of CHIP is able to add an effective E3 function to a U-box-containing client protein.

We postulated that engineered forms of Dorfin could be stable and still function as specific E3s for mutant SOD1s. Dorfin has a RING/IBR domain in the N-terminal portion (amino acids 1-332), but has no obvious motif in the rest of the C-terminus (amino acids 333–838). In this study, we have demonstrated that the hydrophobic domain of Dorfin (amino acids 333–454) is both necessary and sufficient for substrate recruiting (Fig. 2B). In our engineered proteins, the RING/IBR motif of N-terminal Dorfin was replaced by the UPR domain of CHIP, which had strong E3 activity (Murata et al., 2001). Some of the engineered Dorfin-chimeric proteins, such as Dorfin-CHIP$^{D, G, J}$, and ^{L}, were degraded *in vivo* far more slowly than was wild-type Dorfin, indicating that they were capable of being stably presented *in vivo* (Fig. 3). However, Dorfin-CHIP^{G} failed to show strong ubiquitylation activity against SOD1^{G85R} in HEK293 cells. Since Dorfin-CHIP$^{D, J}$, and ^{L} were able to bind to SOD1^{G85R} more strongly than did Dorfin-CHIP^{G}, the binding activity was more important for the E3 activity than for the protein stability.

We next showed that although all of the Dorfin-CHIP chimeric proteins bound to mutant SOD1 *in vivo*, some of them, such as Dorfin-CHIP$^{B, C}$, and ^{I}, bound less than others (Fig. 4A). In HEK293 cells, Dorfin-CHIP$^{D, E, F, J, K}$, and ^{L} ubiquitylated SOD1^{G85R} more effectively than did Dorfin or CHIP; however, in N2a cells only Dorfin-CHIP^{L} had more effective E3 activity than did Dorfin or CHIP. This discrepancy may be due to differences between HEK 293 and N2a cells which could provide slight different environment for the E3 machinery. Therefore, Dorfin-CHIP^{L} was the most potent of the candidate chimeric proteins in degrading mutant SOD1 in the UPS in neuronal cells. We also showed that Dorfin-CHIP^{L} could specifically bind to and ubiquitylate mutant SOD1s but not SOD1^{WT} *in vivo*, as Dorfin had done (Niwa et al., 2002; Ishigaki et al., 2004) (Fig. 5). This observation confirmed that the hydrophobic domain of Dorfin (amino acids 333–454) is responsible for mutant SOD1 recruiting.

Pulse-chase analysis using N2a cells showed that Dorfin-CHIP^{L} degraded SOD1^{G85R} and SOD1^{G93A} more effectively than did Dorfin (Fig. 6). This is compatible with the finding that Dorfin-CHIP^{L} had a greater effect than Dorfin did on the ubiquitylation against mutant SOD1. The cycloheximide assay verified that the degradation ability of Dorfin-CHIP^{L} against SOD1^{G85R} was stronger than that of Dorfin or CHIP in HEK293 cells (data not shown).

Dorfin-CHIP^{L} also reversed SOD1^{G85R}-associated toxicity in N2a cells more effectively than did Dorfin (Fig. 7). This therapeutic effect of Dorfin-CHIP^{L} was expected from its strong E3 activity and degradation ability against SOD1^{G85R}. Visible protein aggregations have been considered to be hallmarks of neurodegeneration. Increased understanding of the pathway involved in protein aggregation may demonstrate that visible macroaggregates represent the end-stage of a molecular cascade of steps rather than a direct toxic insult (Ross and Poirier, 2004). Two facts that Dorfin-CHIP^{L} decreased aggregation formation of SOD1^{G85R} and that this effect was inhibited by a proteasome inhibitor should reflect the ability of Dorfin-CHIP^{L} to degrade mutant SOD1 in the UPS of cells.

Based on our present observations, Dorfin-CHIP^{L}, an engineered chimeric molecule with the hydrophobic substrate-binding domain of Dorfin and the U-box domain of CHIP, had stronger E3 activity against mutant SOD1 than did Dorfin or CHIP. Indeed, it not only degraded mutant SOD1 more effectively than did Dorfin or CHIP but, as compared to Dorfin, produced marked attenuation of mutant SOD1-associated toxicity in N2a cells. This protective effect of Dorfin-CHIP^{L} against mutant SOD1 has potential applications to gene therapy for mutant SOD1 transgenic mice because this protein has a long enough life to allow the constant removal of mutant SOD1 from neurons. Since Dorfin was originally identified as a sporadic ALS-associated molecule (Ishigaki et al., 2002b) and is located in the ubiquitin-positive inclusions of various neurodegenerative diseases (Hishikawa et al., 2003), this molecule is an appropriate candidate for future use in gene therapy not only for familial ALS, but also for sporadic ALS and other neurodegenerative disorders.

So far, most reports on engineered chimera E3s have targeted cancer-promoting proteins. Dorfin-CHIP chimeric proteins are the first chimera E3s to be intended for the treatment of neurodegenerative diseases. Since the accumulation of ubiquitylated proteins in neurons is a pathological hallmark of various neurodegenerative diseases, development of chimera E3s like Dorfin-CHIP^{L}, which can remove unnecessary proteins, is a new therapeutic concept. Further analysis, including transgenic overexpression and vector delivery of Dorfin-CHIP chimeric proteins using ALS animal models will increase our understanding of the potential utility of Dorfin-CHIP chimeric proteins as therapeutic tools.

Acknowledgments

We gratefully thank Dr. Shigetsugu Hatakeyama at Hokkaido University for his advice about the construction of Dorfin-CHIP chimeric proteins. This work was supported by the Nakabayashi Trust for ALS Research; a grant for Center of Excellence (COE) from the Ministry of Education, Culture, Sports, Science and Technology of Japan; and grants from the Ministry of Health, Welfare and Labor of Japan.

Appendix A. Supplementary data

Supplementary data associated with this article can be found, in the online version, at doi:10.1016/j.nbd.2006.09.017.

References

Alves-Rodrigues, A., Gregori, L., Figueiredo-Pereira, M.E., 1998. Ubiquitin, cellular inclusions and their role in neurodegeneration. Trends Neurosci. 21, 516–520.

Bercovich, B., Stancovski, I., Mayer, A., Blumenfeld, N., Laszlo, A., Schwartz, A.L., Ciechanover, A., 1997. Ubiquitin-dependent degradation of certain protein substrates in vitro requires the molecular chaperone Hsc70. J. Biol. Chem. 272, 9002–9010.

Ciechanover, A., Brundin, P., 2003. The ubiquitin proteasome system in

neurodegenerative diseases: sometimes the chicken, sometimes the egg. Neuron 40, 427–446.

Cudkowicz, M.E., McKenna-Yasek, D., Sapp, P.E., Chin, W., Geller, B., Hayden, D.L., Schoenfeld, D.A., Hosler, B.A., Horvitz, H.R., Brown, R.H., 1997. Epidemiology of mutations in superoxide dismutase in amyotrophic lateral sclerosis. Ann. Neurol. 41, 210–221.

Glickman, M.H., Ciechanover, A., 2002. The ubiquitin–proteasome proteolytic pathway: destruction for the sake of construction. Physiol. Rev. 82, 373–428.

Hatakeyama, S., Matsumoto, M., Kamura, T., Murayama, M., Chui, D.H., Planel, E., Takahashi, R., Nakayama, K.I., Takashima, A., 2004. U-box protein carboxyl terminus of Hsc70-interacting protein (CHIP) mediates poly-ubiquitylation preferentially on four-repeat Tau and is involved in neurodegeneration of tauopathy. J. Neurochem. 91, 299–307.

Hatakeyama, S., Watanabe, M., Fujii, Y., Nakayama, K.I., 2005. Targeted destruction of c-Myc by an engineered ubiquitin ligase suppresses cell transformation and tumor formation. Cancer Res. 65, 7874–7879.

Hishikawa, N., Niwa, J., Doyu, M., Ito, T., Ishigaki, S., Hashizume, Y., Sobue, G., 2003. Dorfin localizes to the ubiquitylated inclusions in Parkinson's disease, dementia with Lewy bodies, multiple system atrophy, and amyotrophic lateral sclerosis. Am. J. Pathol. 163, 609–619.

Ishigaki, S., Liang, Y., Yamamoto, M., Niwa, J., Ando, Y., Yoshihara, T., Takeuchi, H., Doyu, M., Sobue, G., 2002a. X-Linked inhibitor of apoptosis protein is involved in mutant SOD1-mediated neuronal degeneration. J. Neurochem. 82, 576–584.

Ishigaki, S., Niwa, J., Ando, Y., Yoshihara, T., Sawada, K., Doyu, M., Yamamoto, M., Kato, K., Yotsumoto, Y., Sobue, G., 2002b. Differentially expressed genes in sporadic amyotrophic lateral sclerosis spinal cords—Screening by molecular indexing and subsequent cDNA microarray analysis. FEBS Lett. 531, 354–358.

Ishigaki, S., Hishikawa, N., Niwa, J., Iemura, S., Natsume, T., Hori, S., Kakizuka, A., Tanaka, K., Sobue, G., 2004. Physical and functional interaction between Dorfin and Valosin-containing protein that are colocalized in ubiquitylated inclusions in neurodegenerative disorders. J. Biol. Chem. 279, 51376–51385.

Ito, T., Niwa, J., Hishikawa, N., Ishigaki, S., Doyu, M., Sobue, G., 2003. Dorfin localizes to Lewy bodies and ubiquitylates synphilin-1. J. Biol. Chem. 278, 29106–29114.

Johnston, J.A., Ward, C.L., Kopito, R.R., 1998. Aggresomes: a cellular response to misfolded proteins. J. Cell Biol. 143, 1883–1898.

Julien, J.P., 2001. Amyotrophic lateral sclerosis. unfolding the toxicity of the misfolded. Cell 104, 581–591.

Jungmann, J., Reins, H.A., Schobert, C., Jentsch, S., 1993. Resistance to cadmium mediated by ubiquitin-dependent proteolysis. Nature 361, 369–371.

Lee, D.H., Sherman, M.Y., Goldberg, A.L., 1996. Involvement of the molecular chaperone Ydj1 in the ubiquitin-dependent degradation of short-lived and abnormal proteins in *Saccharomyces cerevisiae*. Mol. Cell. Biol. 16, 4773–4781.

Meacham, G.C., Patterson, C., Zhang, W., Younger, J.M., Cyr, D.M., 2001. The Hsc70 co-chaperone CHIP targets immature CFTR for proteasomal degradation. Nat. Cell Biol. 3, 100–105.

Miyazaki, K., Fujita, T., Ozaki, T., Kato, C., Kurose, Y., Sakamoto, M., Kato, S., Goto, T., Itoyama, Y., Aoki, M., Nakagawara, A., 2004. NEDL1, a novel ubiquitin–protein isopeptide ligase for dishevelled-1, targets mutant superoxide dismutase-1. J. Biol. Chem. 279, 11327–11335.

Murata, S., Minami, Y., Minami, M., Chiba, T., Tanaka, K., 2001. CHIP is a chaperone-dependent E3 ligase that ubiquitylates unfolded protein. EMBO Rep. 2, 1133–1138.

Murata, S., Chiba, T., Tanaka, K., 2003. CHIP: a quality-control E3 ligase collaborating with molecular chaperones. Int. J. Biochem. Cell Biol. 35, 572–578.

Niwa, J., Ishigaki, S., Doyu, M., Suzuki, T., Tanaka, K., Sobue, G., 2001. A novel centrosomal ring-finger protein, dorfin, mediates ubiquitin ligase activity. Biochem. Biophys. Res. Commun. 281, 706–713.

Niwa, J., Ishigaki, S., Hishikawa, N., Yamamoto, M., Doyu, M., Murata, S., Tanaka, K., Taniguchi, N., Sobue, G., 2002. Dorfin ubiquitylates mutant SOD1 and prevents mutant SOD1-mediated neurotoxicity. J. Biol. Chem. 277, 36793–36798.

Oyake, D., Nishikawa, H., Koizuka, I., Fukuda, M., Ohta, T., 2002. Targeted substrate degradation by an engineered double RING ubiquitin ligase. Biochem. Biophys. Res. Commun. 295, 370–375.

Rosen, D.R., Siddique, T., Patterson, D., Figlewicz, D.A., Sapp, P., Hentati, A., Donaldson, D., Goto, J., O'Regan, J.P., Deng, H.X., et al., 1993. Mutations in Cu/Zn superoxide dismutase gene are associated with familial amyotrophic lateral sclerosis. Nature 362, 59–62.

Ross, C.A., Poirier, M.A., 2004. Protein aggregation and neurodegenerative disease. Nat. Med. 10, S10–S17 (Suppl.).

Rowland, L.P., Shneider, N.A., 2001. Amyotrophic lateral sclerosis. N. Engl. J. Med. 344, 1688–1700.

Sakamoto, K.M., Kim, K.B., Kumagai, A., Mercurio, F., Crews, C.M., Deshaies, R.J., 2001. Protacs: chimeric molecules that target proteins to the Skp1-Cullin-F box complex for ubiquitination and degradation. Proc. Natl. Acad. Sci. U. S. A. 98, 8554–8559.

Sakamoto, K.M., Kim, K.B., Verma, R., Ransick, A., Stein, B., Crews, C.M., Deshaies, R.J., 2003. Development of Protacs to target cancer-promoting proteins for ubiquitination and degradation. Mol. Cell Proteomics 2, 1350–1358.

Scheffner, M., Nuber, U., Huibregtse, J.M., 1995. Protein ubiquitination involving an E1–E2–E3 enzyme ubiquitin thioester cascade. Nature 373, 81–83.

Sherman, M.Y., Goldberg, A.L., 2001. Cellular defenses against unfolded proteins: a cell biologist thinks about neurodegenerative diseases. Neuron 29, 15–32.

Shimura, H., Schwartz, D., Gygi, S.P., Kosik, K.S., 2004. CHIP–Hsc70 complex ubiquitinates phosphorylated tau and enhances cell survival. J. Biol. Chem. 279, 4869–4876.

Tanaka, K., Suzuki, T., Hattori, N., Mizuno, Y., 2004. Ubiquitin, proteasome and parkin. Biochim. Biophys. Acta 1695, 235–247.

Urushitani, M., Kurisu, J., Tateno, M., Hatakeyama, S., Nakayama, K., Kato, S., Takahashi, R., 2004. CHIP promotes proteasomal degradation of familial ALS-linked mutant SOD1 by ubiquitinating Hsp/Hsc70. J. Neurochem. 90, 231–244.

Yoshida, Y., Tokunaga, F., Chiba, T., Iwai, K., Tanaka, K., Tai, T., 2003. Fbs2 is a new member of the E3 ubiquitin ligase family that recognizes sugar chains. J. Biol. Chem. 278, 43877–43884.

Gene Expression Profiling toward Understanding of ALS Pathogenesis

FUMIAKI TANAKA, JUN-ICHI NIWA, SHINSUKE ISHIGAKI, MASAHISA KATSUNO, MASAHIRO WAZA, MASAHIKO YAMAMOTO, MANABU DOYU, AND GEN SOBUE

Department of Neurology, Nagoya University Graduate School of Medicine, 65 Tsurumai-cho, Showa-ku, Nagoya 466-8550, Japan

ABSTRACT: **Although more than 130 years have gone by since the first description in 1869 by Jean-Martin Charcot, the mechanism underlying the characteristic selective motor neuron degeneration in amyotrophic lateral sclerosis (ALS) has remained elusive. Modest advances in this research field have been achieved by the identification of copper/zinc superoxide dismutase 1 (SOD1) as one of the causative genes for rare familial ALS (FALS) and by the development and analysis of mutant SOD1 transgenic mouse models. However, in sporadic ALS (SALS) with many more patients, causative or critical genes situated upstream of the disease pathway have not yet been elucidated and no available disease models have been established. To approach genes causative or critical for ALS, gene expression profiling in tissues primarily affected by the disease has represented an attractive research strategy. We have been working on screening these genes employing and combining several new technologies such as cDNA microarray, molecular indexing, and laser capture microdissection. Many of the resultant genes are of intense interest and may provide a powerful tool for determining the molecular mechanisms of ALS. However, we have barely arrived at the starting point and are confronting an enormous number of genes whose roles remain undetermined. Challenging tasks lie ahead of us such as identifying which genes are really causative for ALS and developing a disease model of SALS with due consideration for the expression changes in those genes.**

KEYWORDS: **ALS; SOD1; gene expression analysis; cDNA microarray; molecular indexing; laser capture microdissection**

INTRODUCTION

Amyotrophic lateral sclerosis (ALS) is a neurodegenerative and fatal human disorder characterized by loss of motor neurons in the spinal cord, brain stem,

Address for correspondence: Dr. Gen Sobue, Department of Neurology, Nagoya University Graduate School of Medicine, 65 Tsurumai-cho, Showa-ku, Nagoya 466-8550, Japan. Voice: +81-52-744-2385; fax: +81-52-744-2384.
e-mail: sobueg@med.nagoya-u.ac.jp

Ann. N.Y. Acad. Sci. 1086: 1–10 (2006).
doi: 10.1196/annals.1377.011

and motor cortex, presenting as weakness of the limbs, speech abnormalities, and difficulties in swallowing.[1] The terminal phases of the disease involve respiratory insufficiency and half of the patients die within 3 years after the onset of symptoms. ALS can be inherited as an autosomal dominant trait in a subset of individuals who make up 5% to 10% of the total population of those affected. In addition, 20% to 30% of familial ALS (FALS) cases are associated with a mutation in the copper/zinc superoxide dismutase 1 gene (SOD1).[2] However, more than 90% of ALS patients are sporadic, not showing any familial trait. Since there have been no available disease models for sporadic ALS (SALS) as of now, transgenic mouse models or cell culture models[3] of ALS associated with SOD1 mutations have proven very useful in studying the initial mechanisms underlying this neurodegenerative disease of unknown etiology. The use of an animal model makes it possible and easy to investigate the different stages of disease progression including the early preclinical phase.

One of the experimental approaches toward a more comprehensive understanding of the molecular changes occurring in ALS is gene expression study[4] employing array-based methods or a differential display and its related techniques. Using transgenic mouse models expressing the SOD1 gene with a G93A mutation, we performed cDNA microarray analysis[5] to reveal the transcriptional profiles of affected tissues, namely, spinal anterior horn tissues. This analysis revealed an upregulation of genes related to an inflammatory process together with a change in apoptosis-related gene expression at the presymptomatic stage prior to motor neuron death.

Next, we extended our gene expression study from mouse to human postmortem spinal anterior horn tissues obtained from SALS patients. In this analysis, we employed a molecular indexing technique, a modified version of the differential display developed by Kato in 1995.[6] These PCR-based screening procedures have the advantage of being able to cover an unrestricted range of expressed genes including even hitherto unknown ones. As a result, we have successfully cloned a novel gene designated "dorfin,"[7] the expression of which was upregulated in SALS spinal cords.

Using spinal anterior horn tissues of SOD1 mutant mice or SALS patients as starting materials, these gene expression studies[5,7] have shed considerable light on the pathogenesis of FALS and SALS. However, in the spinal anterior horn tissues of ALS spinal cords, there are reduced numbers of motor neurons with glial cell proliferation. The alteration of the gene expression in the spinal anterior horn tissues could reflect the number of motor neurons and glial cells during disease progression. Such a disadvantage in using anterior horn tissues as starting materials prompted us to try to extract a pure motor neuron-specific gene expression profile. To this end, we employed the technology of laser capture microdissection[8] combined with T7-based RNA amplification and cDNA microarrays, which culminated in the successful detection of a total of 196 genes considered important for the SALS molecular mechanism.[9]

GENE EXPRESSION ANALYSIS FOR MUTANT SOD1 MOUSE MODEL OF ALS

We analyzed both temporal and differential gene expressions in the lumbar spinal anterior horn tissues of the transgenic mouse models expressing the SOD1 gene with a G93A mutation and the controls.[5] In this analysis, we detected a significant upregulation of 30 specific transcripts and downregulation of 7 transcripts in the spinal cords of mutant SOD1 mice[5] (TABLE 1). Before 11 weeks of age, mutant SOD1 mice are free of a disease phenotype, but they begin to decline rapidly in motor function after 14 weeks. The employment of mice for gene expression analysis provides a great advantage in obtaining data in the preclinical stage.

Interestingly, we found an upregulation of genes related to an inflammatory process together with a change in apoptosis-related gene expression at 11 weeks of age in the preclinical stage prior to motor neuron death.[5] The representative inflammatory-related genes elevated in their expression at this stage were the tumor necrosis factor (TNF)-α gene, which is a proinflammatory cytokine, and the Janus tyrosine-protein kinase 3 (JAK3), a necessary component of cytokine receptor signaling (TABLE 1). At a subsequent disease stage of 14 or 17 weeks of age, many more genes associated with an inflammatory process such as cathepsin D, serine protease inhibitor (SPI) 2–4, and cystatin C precursor, CD68, CD147, and clusterin increased their expression (TABLE 1). A histopathological evaluation showed glial cell activation and proliferation as early as 11 weeks of age and continuing to advance until 17 weeks.[10] A temporal increase in the expression level observed in these genes might reflect an inflammatory response with activated microglia and reactive astrocytes.

On the other hand, caspase-1, an initiator of the neuronal apoptotic cascade, was also upregulated at a presymptomatic 11 weeks of age (TABLE 1). An interrelationship between the inflammatory reaction and apoptotic pathway has been demonstrated. In addition to its role as an initiator of neuronal apoptotis, extracellular caspase-1 converts interleukin-1β (IL-1β) into a mature form. Thus, caspase-1 activation in motor neurons contributes to an inflammatory pathway with early astrocytosis and microglial activation in mutant SOD1 mice. In contrast, there is strong evidence for an inflammatory response involving microglial activation that leads to neuronal apoptosis.[11] Activated microglia express neurotoxic cytokines and substances such as TNF-α, proteases, oxyradicals, and small reactive molecules.[12] A nearly simultaneous upregulation of genes related to an inflammatory process and apoptotic initiation at the preclinical stage might contribute to the relentless neurodegenerative process making for a detrimental cycle. At 14 weeks of age, an early phase of the symptomatic stage, a key executioner of apoptosis, caspase-3, resulting from caspase-1 activation, began to be upregulated.[13] This finding agrees with